การออกแบบตัวควบคุมความถี่เนื่องจากโหลด
สำหรับระบบไฟฟ้ากำลังภายใต้การรบกวนแบบคงอยู่ที่มีขอบเขตจำกัด

นายปฏิภาณ กาลวิบูลย์

วิทยานิพนธ์นี้เป็นส่วนหนึ่งของการศึกษาตามหลักสูตรปริญญาวิศวกรรมศาสตรมหาบัณฑิต
สาขาวิชาวิศวกรรมไฟฟ้า ภาควิชาวิศวกรรมไฟฟ้า
คณะวิศวกรรมศาสตร์ จุฬาลงกรณ์มหาวิทยาลัย
ปีการศึกษา ๒๕๕๘

DESIGN OF LOAD FREQUENCY CONTROLLER FOR POWER SYSTEMS SUBJECT TO BOUNDED PERSISTENT DISTURBANCES

Mr Patipan Kalvibool

A Thesis Submitted in Partial Fulfillment of the Requirements

for the Degree of Master of Engineering Program in Electrical Engineering

Department of Electrical Engineering

Faculty of Engineering

Chulalongkorn University

Academic Year 2015

Thesis Title	DESIGN OF LOAD FREQUENCY CONTROLLER FOR POWER SYSTEMS SUBJECT TO BOUNDED PERSISTENT DISTURBANCES
By	Mr Patipan Kalvibool
Field of Study	Electrical Engineering
Thesis Advisor	Assistant Professor Suchin Arunsawatwong, PhD

Accepted by the Faculty of Engineering, Chulalongkorn University in Partial Fulfillment of the Requirements for the Master's Degree

. . . . . Dean of the Faculty of Engineering
(Professor Bundhit Eua-Arporn, PhD)

THESIS COMMITTEE

. . . . . Chairman
(Assistant Professor Somboon Sangwongwanich, PhD)

. . . . . Thesis Advisor
(Assistant Professor Suchin Arunsawatwong, PhD)

. . . . . Examiner
(Assistant Professor Naebboon Hoonchareon, PhD)

. . . . . External Examiner
(Professor Issarachai Ngamroo, PhD)

ปฏิภาณ กาลวิบูลย์: การออกแบบตัวควบคุมความถี่เนื่องจากโหลดสำหรับระบบไฟฟ้ากำลังภายใต้การรบกวนแบบคงอยู่ที่มีขอบเขตจำกัด (DESIGN OF LOAD FREQUENCY CONTROLLER FOR POWER SYSTEMS SUBJECT TO BOUNDED PERSISTENT DISTURBANCES), อ.ที่ปรึกษาวิทยานิพนธ์: ผศ. ดร.สุชิน อรุณสวัสดิ์วงศ์, ๖๘ หน้า.

รูปคลื่นของกำลังงานไฟฟ้าที่ผลิตขึ้นจากแหล่งพลังงานหมุนเวียน เช่น ลม แสงอาทิตย์ มีลักษณะไม่แน่นอน และบ่อยครั้งแปรเปลี่ยนแบบคงอยู่เป็นระยะเวลานาน วิทยานิพนธ์นี้นำเสนอการออกแบบตัวควบคุมความถี่เนื่องจากโหลดสำหรับระบบไฟฟ้ากำลังซึ่งทำงานภายใต้การรบกวนแบบคงอยู่ โดยใช้หลักอสมการและหลักการเข้าคู่ วัตถุประสงค์หลักของการออกแบบคือ การรับประกันว่า ขนาดของสัญญาณขาออกที่สนใจมีค่าอยู่ในขอบเขตที่ยอมรับได้อย่างเคร่งครัดตลอดเวลาและต่อทุกสัญญาณรบกวนทั้งหมดที่เป็นไปได้ ประโยชน์หนึ่งของกรอบงานที่นำมาใช้คือ เมื่อพบคำตอบของการออกแบบแล้ว เราสามารถรับประกันได้ว่า ระบบจะปฏิบัติการด้วยระดับความปลอดภัยที่น่าพอใจและการจ่ายพลังงานมีคุณภาพ กรณีศึกษาสองกรณีถูกจัดทำขึ้น ผลการจำลองเชิงเลขแสดงให้เห็นอย่างชัดเจนว่า กรอบงานที่นำมาใช้ในงานนี้มีความเหมาะสมและมีประสิทธิผล ดังนั้นการกำหนดรูปแบบปัญหาจึงเป็นไปอย่างสมจริง

ภาควิชา . . . วิศวกรรมไฟฟ้า . . . ลายมือชื่อนิสิต . . . . . .

สาขาวิชา . . . วิศวกรรมไฟฟ้า . . . ลายมือชื่ออ.ที่ปรึกษาหลัก . . . . . .

ปีการศึกษา . . . . ๒๕๕๘ . . . .

##557 05501 21: MAJOR ELECTRICAL ENGINEERING
KEYWORDS: POWER SYSTEMS / LOAD FREQUENCY CONTROL / PERSISTENT DISTURBANCE / PRINCIPLE OF INEQUALITIES / PRINCIPLE OF MATCHING

PATIPAN KALVIBOOL: DESIGN OF LOAD FREQUENCY CONTROLLER FOR POWER SYSTEMS SUBJECT TO BOUNDED PERSISTENT DISTURBANCES.
ADVISOR: ASSISTANT PROFESSOR SUCHIN ARUNSAWATWONG, PhD, 68 pp.

The waveforms of the electric power generated from renewable energy sources such as wind and sunlight are known to be uncertain and, very often, vary persistently for a long period of time. This thesis presents the design of load frequency controllers for power systems that are subject to persistent disturbances by using the principle of inequalities and the principle of matching. The principal design objective is to guarantee that the magnitudes of the outputs of interest always stay strictly within their acceptable bounds for all time in the presence of all the possible disturbances. An advantage of the framework adopted here is that once a solution is found, the system is guaranteed to operate with satisfactory levels of security and quality supply. Two case studies have been carried out; the numerical results clearly show that the framework adopted here is suitable and effective, thereby giving a realistic formulation of the design problem.

Department: .... Electrical Engineering .... Student's Signature .....
Field of Study: ... Electrical Engineering ... Advisor's Signature .....
Academic Year .....2015.....

ACKNOWLEDGEMENTS

A thesis is a crystallization of a person's work. An interesting part of the thesis is not in its contents but in the story on how it evolves from the very first letter to its final form. However, the development of the thesis cannot be done solely by oneself. It is influenced, raised, and nourished by several people. First and foremost, I would like to express my deepest gratitude to my advisor Assistant Professor Suchin Arunsawatwong, who has patiently tutored me and given me invaluable advice and wisdom in both academic and personal aspects since I was an undergraduate student at the department of electrical engineering, Chulalongkorn University.

Also, I would like to express my gratitude to Assistant Professor Somboon Sangwongwanich for providing me with some background on battery energy storage system and kindly serving on the thesis committee as a chairman. I am thankful for Assistant Professor Naebboon Hoonchareon who introduces me to the field of power system dynamics and stability and becomes one of the committees. I also express my gratitude to Professor Issarachai Ngamroo for his willingness to serve on the thesis committee.

Thanks are also given to all people, past and present, in Control Systems Research Laboratory (CSRL) at Chulalongkorn University for their support, encouragement, and friendship. I appreciate that they are very approachable and kind. They helped and supported me through the difficult time of study and coursework.

Last but not least, for a person to direct his zeal to the pilgrimage of knowledge, several others have to sacrifice their invaluable resource to support the person. I would like to thank my family for their unconditional understanding, extensive support and unceasing love. Much of their serenity is sacrificed in the dark hours where the author spent days and nights cultivating the fruit of wisdom. They will everlastingly hold a place in my heart.

CONTENTS

Chapter Page

LIST OF TABLES

LIST OF FIGURES

CHAPTER I

INTRODUCTION

1.1 Motivation

Nowadays, the use of renewable energy produced from sources such as wind and sunlight becomes more significant in power generation [8,22,36]. The waveforms of the power generated from such renewable energy sources are known to be highly uncertain and, very often, vary persistently for a long period of time, e.g., Figure 1.1 and Figure 1.2 (taken from [4] and [21], respectively).

In power system operation, any mismatch between generation and load causes the system frequency to deviate from its nominal value. When the system frequency deviates too far from the nominal value for a rather long period of time, it can cause severe problems to the overall power system. If the system frequency can be guaranteed to stay strictly within acceptable range for all time during operation, the power system will operate with satisfactory levels of security and quality supply.

As suggested by [6], designing a load frequency controller for power systems subject to persistent disturbances generated by renewable energy sources is a challenging design problem. This is because conventional design formulations are based on deterministic test signals (e.g., step and sinusoidal functions) and are hardly related to the uncertain characteristic of such disturbances. Fortunately, the problem can be solved successfully by using Zakian's framework [44,45]. The framework consists of two design principles: namely, the method of inequalities [42, 44, 46] and the principle of matching [42–44]. See Chapter 3 for further discussion.

1.2 Literature Review

The design of controllers for load frequency control (LFC) of power systems has been investigated by many researchers (see, e.g., [3, 11–13, 15–17, 20, 22, 33, 36, 41]). Since there are

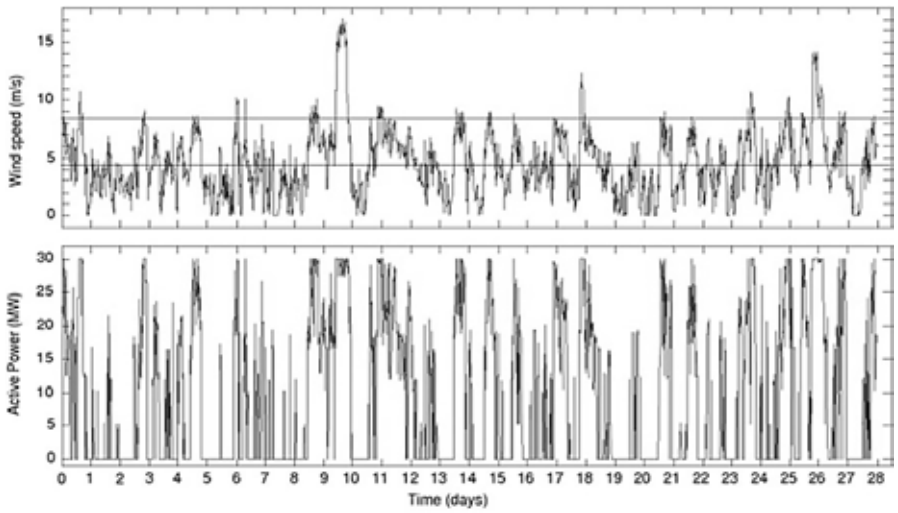

Figure 1.1: One month waveforms of (top) wind speed and (bottom) the real power produced by a wind farm [4]

a number of articles on this subject, readers are referred to survey papers, e.g., [22, 36] and the references therein. It should be noted that the design formulations used by many researchers consider the case in which the loads are assumed to be deterministic test inputs (e.g., step functions or sinusoids). Some of them are as follows.

- Ćalović [11] proposes the linear regulator design for LFC based on centralized optimal linear quadratic (LQ) regulator theory. Moreover, in [12], he proposes a decentralized scheme for automatic generation control (AGC) by using the optimal LQ regulators whereas in [13], he proposes the addition of tie-line loss compensation to the standard conventional control algorithm. All of the above papers consider the cases in which the disturbances are assumed to be step functions.

- Davison and Tripathi [17] propose the optimal decentralized control for LFC of multi-area interconnected power systems using a parameter optimization method. The numerical optimization technique is used to minimize the dominant time constant of the closed-loop system subject to nonlinear constraints that represent desirable properties of the system. In the design formulation used in their work, the exogenous input (disturbance) is assumed to be unknown constant.

- Feliachi [20] proposes the methodology for feasibility analysis and design of optimal de-

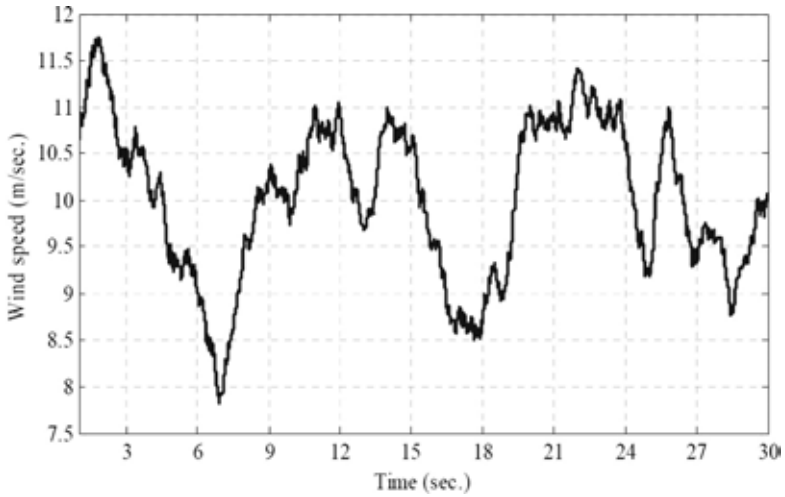

Figure 1.2: Waveform of wind speed up to 30 seconds [21]

centralized controller for LFC. The design formulation is expressed in terms of eigenvalue sensitivities. The design is verified by considering the system responses due to step disturbances.

- Chidambaram and Velusami [15] propose a design of biased controllers for the decentralized LFC of interconnected power systems. They use the well-known integral squared error (ISE) criterion in conjunction with the maximum stability margin (MSM) criterion where the disturbance is assumed to be a step function.

- Recently, Alrifai *et al.* [3] develop the design of decentralized controller for LFC based on overlapped decomposition. However, their design schemes involve the optimization of the system's transient responses due to step disturbances.

Apparently, Miniesy and Bohn [33] make an acknowledgement that load change in power systems is not always known in advance. In this connection, they employ the differential approximation technique and Luenberger type observer to estimate the load disturbance acting on the system in such a way that the optimum control technique can be used for the case in which load disturbances change rapidly. Unfortunately, when the load fluctuates persistently in a random manner, such control theories no longer provide effective tools for designing controllers for the power system.

1.3 Thesis Objective

The purpose of this thesis is to design controllers for LFC of power systems operating under persistent disturbances. The design framework adopted in the thesis has been developed by Zakian [42–46] and his group (see [45] for a comprehensive list of references), which consists of two design principles: namely, the principle of inequalities and the principle of matching. The principal design objective is to ensure that the outputs of interest are always kept within acceptable ranges for all time and for all possible input so that the power system is guaranteed to operate with a satisfactory level of security and quality supply.

1.4 Scope of Thesis

- The power system dynamic model used in the thesis is a linearized state-space model, assuming small variation of variables and separation of the real power and frequency behaviour from the phenomena connected with reactive power and voltage.
- For two-area power system, the coupling effects among parallel operated synchronous generating units within the same area are neglected so that each area has a single frequency.
- The disturbances that are treated in this study are bounded persistent change in load and can therefore be modelled appropriately as signals having uniform bounds on both magnitude and slope.

1.5 Methodology

1. Collect and study literature on LFC design problems.
2. Employ the principle of matching and the method of inequalities to the design problem so that the change in load is explicitly taken as signals having uniform bounds on magnitude and slope and the design specifications are explicitly expressed as a set of inequalities that can be solved in practice.
3. Solve the design problem and obtain the solution that satisfies all of the inequalities simultaneously.

1.6 Contributions

- A methodology of controller design for LFC of power systems operating under persistent disturbances (see Chapter 4 and Chapter 5).
- Case studies of controller design for LFC of power systems subject to bounded persistent disturbances (see Chapter 4 and Chapter 5).
- Computer software for the case studies.

1.7 Structure of Thesis

The organization of the thesis is as follows. In Chapter 2, the basic concepts of electric power system operation and control are briefly explained. Chapter 3 recapitulates the design theory used in the thesis. Chapter 4 presents the controller design for LFC of two-area interconnected power system. Chapter 5 presents the controller design for LFC when the generation rate constraint is taken into consideration and the benefit of using battery energy storage system in the LFC system is illustrated as well. Finally, conclusions are given in Chapter 6.

CHAPTER II

BASIC CONCEPTS OF ELECTRIC POWER SYSTEM OPERATION AND CONTROL

Since electric power system is a vast field, this chapter briefly explains only the concepts of electric power system control that are related to the thesis. The details can be found in standard textbooks, e.g., [28, 29].

In §2.1, the concepts of electric power system operation and control are explained. The basic concepts of the load frequency control and the generation rate constraint are presented in §2.2. In §2.3, the information about the battery energy storage system associated with the LFC is provided.

2.1 Electric Power System Operation and Control

An electric power system converts energy from one of the naturally available forms to the electrical form and transmits that electrical energy to the points of consumption. The advantage of doing so is that the electrical energy can be transmitted and controlled with relative ease and with a high degree of efficiency and reliability. In this regard, a properly designed and operated power system should meet the following fundamental requirements [29]:

1. The system must be able to meet the continually changing load for real and reactive power. Since the electricity cannot be conveniently stored in sufficient quantities, the real and reactive power should be maintained and appropriately controlled at all times.
2. The system should supply energy at a minimal cost and with minimal amount of ecological impact.
3. The quality of power supply must meet certain minimum standards with regard to the following factors:
    - constancy of frequency,
    - constancy of voltage, and

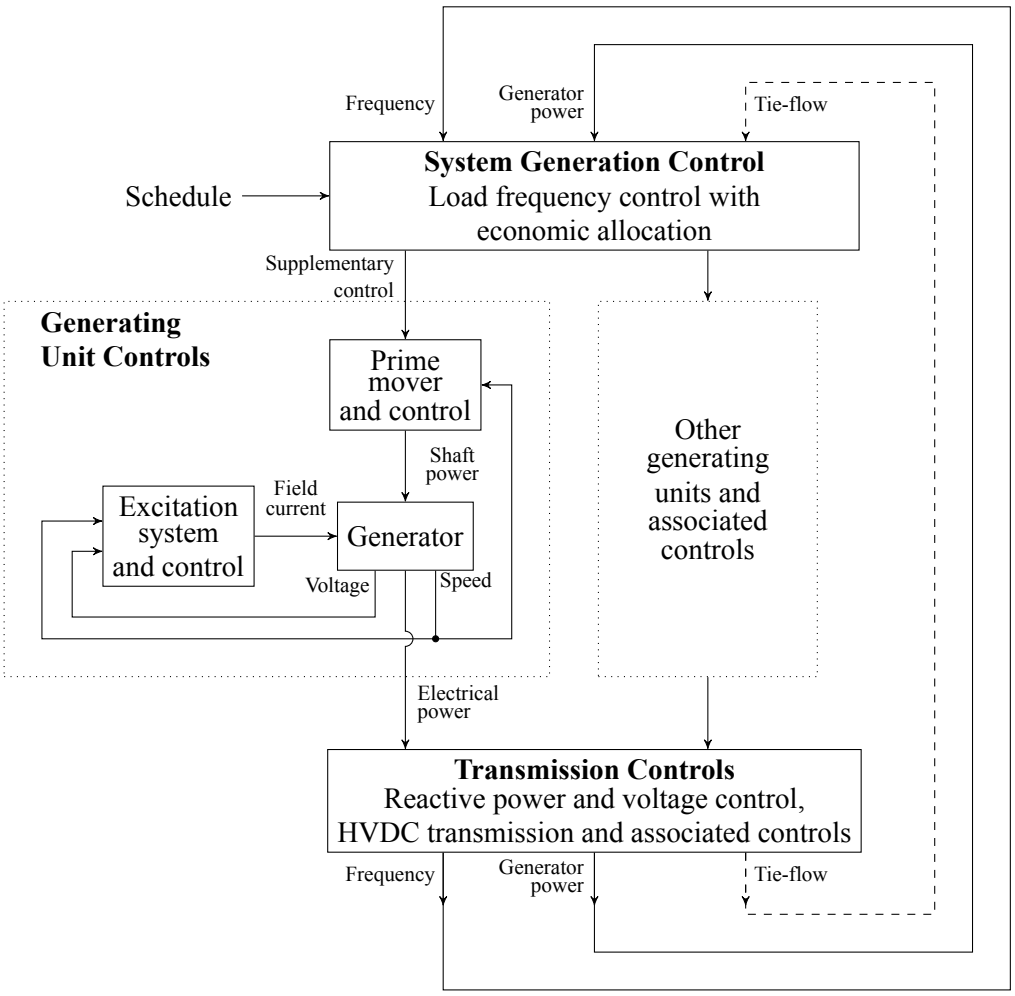

Figure 2.1: Subsystems of a power system and associated controls

- level of reliability.

Several levels of controls involving a complex array of devices are used to meet the above requirements. Figure 2.1 identifies various subsystems of a power system and the associated controls. In this overall structure, there are controllers operating directly on individual system elements. These are briefly explained as follows.

- A generating unit consists of a prime mover control loop and an excitation control loop. The former one is concerned with speed regulation and control of energy supply system variables such as boiler pressures, temperatures, and flows. On the other hand, the function of the excitation control loop is to regulate generator voltage and reactive power output.

The desired power outputs of the individual generating units are determined by the system generation control.

- The primary purpose of the system generation control or automatic generation control (AGC) is to balance the total system generation against the system load and losses so that the desired frequency and the balance of generation and consumption are maintained. For the interconnected power system, the power interchange with neighbouring systems (tie-flows) also needs to be maintained.
- The transmission controls include power and voltage control devices, such as static var compensators, synchronous condensers, switched capacitors and reactors, tap-changing transformers, phase-shifting transformers, and HVDC transmission controls.

The controls described above contribute to the satisfactory operation of the power system by maintaining system variables (e.g., frequency, voltages) within their acceptable limits. They also have a profound effect on the dynamic performance of the power system and on its ability to cope with disturbances.

The control objectives are dependent on the operating state of the power system. Under normal conditions, the control objective is to operate as efficiently as possible with voltages and frequency close to nominal values. When an abnormal condition develops, new objectives must be met to restore the system to normal operation.

From the control-theoretical point of view, a power system is a very high-order multivariable system operating in constantly changing environments. Because of the high dimensionality and complexity of the system, it is essential to make simplifying assumptions and to use the right degree of detail of the system representation to analyze specific problem. This requires a good grasp of the characteristics of the overall system.

In the thesis, only the real power and frequency control, which is commonly referred to as load frequency control (LFC), is discussed. It should also be noted that, from now on, the word ‘power’ alone throughout this thesis is referred to as the ‘real power.’

2.2 Load Frequency Control (LFC)

It is known (see, e.g., [28, 29]) that the frequency of a system is dependent on real power balance. As frequency is a common factor throughout the system, a change in real power at one point is reflected throughout the system by a change in frequency. From Figure 2.1, one can see that load frequency control (LFC) is a supplementary control for manipulating the power generation of the system.

As previously mentioned, the frequency of a system depends on the real power balance. This is because of the synchronous machine characteristic which generally is the main generating unit in a power system. A mismatch between generation and consumption, in a point of view of synchronous generator, is a mismatch between electrical power and mechanical power. When there is such a mismatch, it will cause the rotor speed to deviate from its nominal value. This can be seen obviously from the swing equation:

$$2H\frac{d\omega_r}{dt} = T_m - T_e \tag{2.1}$$

where H is the inertia constant, ω_r the rotor speed, T_m and T_e mechanical and electrical torques, respectively. Since the rotor speed is directly related to the frequency of the electrical output, the mismatch between the generation and the consumption will cause the system frequency to deviate from the nominal value.

Basically, in synchronous generators, there is a basic controller (or regulator) known as governor that regulates the speed of the rotor. The LFC loop sends a supplementary control signal to the governor in order to improve the speed regulation (and hence frequency regulation) and restore the system frequency to its nominal value.

The basic concepts of LFC can clearly be illustrated by considering a single area power system. This is discussed in the next subsection.

2.2.1 LFC for single area power system

With primary speed control (from the governor action), a change in system load will result in a steady-state frequency deviation. All generating units will contribute to the overall change in

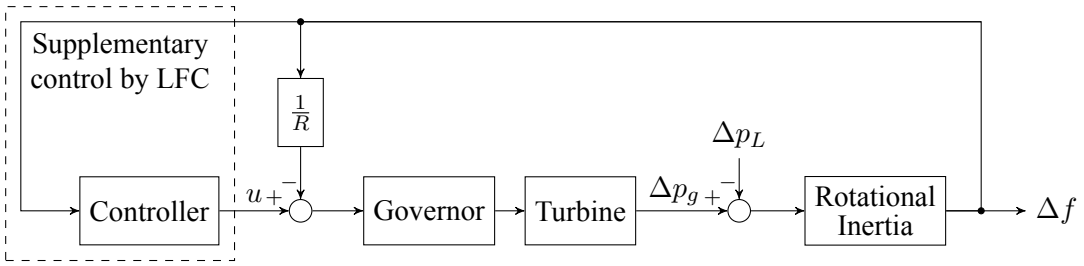

R is speed regulation of the governor
u is the supplementary control signal
Δp_g is the generation power deviation
Δp_L is the load deviation
Δf is the frequency deviation

Figure 2.2: Block diagram of LFC for a single area power system with supplementary control

the power generation, irrespective of the location of the load change. Restoration of the system frequency to its nominal value requires supplementary control which adjusts the load reference setpoint. Therefore, the basic objective of controlling prime-mover power to match the variations in the system load in a desired manner is through control of the load reference setpoints of selected generating units. As the system load is continually changing, it is necessary to control the output of generators automatically.

The block diagram shown in Figure 2.2 is a conventional LFC for a single area power system. It uses the frequency deviation as an output signal fed back to the controller. Generally, the conventional controller for LFC is the integral controller which has the transfer function:

$$K_I(s) = \frac{k_I}{s} \tag{2.2}$$

where k_I is an integral gain.

It should be noted that, normally, the coupling effects among parallel operated synchronous generating units within an area are neglected so that the area has single frequency.

2.2.2 LFC for two-area interconnected power system

When two or more independent power systems are connected, they exchange and share the power between the neighbouring systems via tie-line. Thus, for interconnected power systems, the tie-flow is taken into consideration so that the quality and the efficiency of exchange and

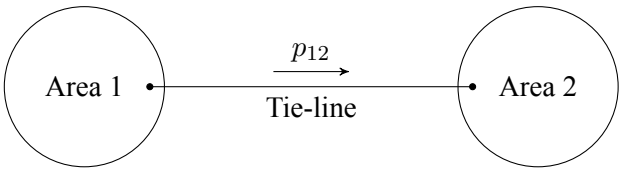

Figure 2.3: Schematic diagram of two-area interconnected power system

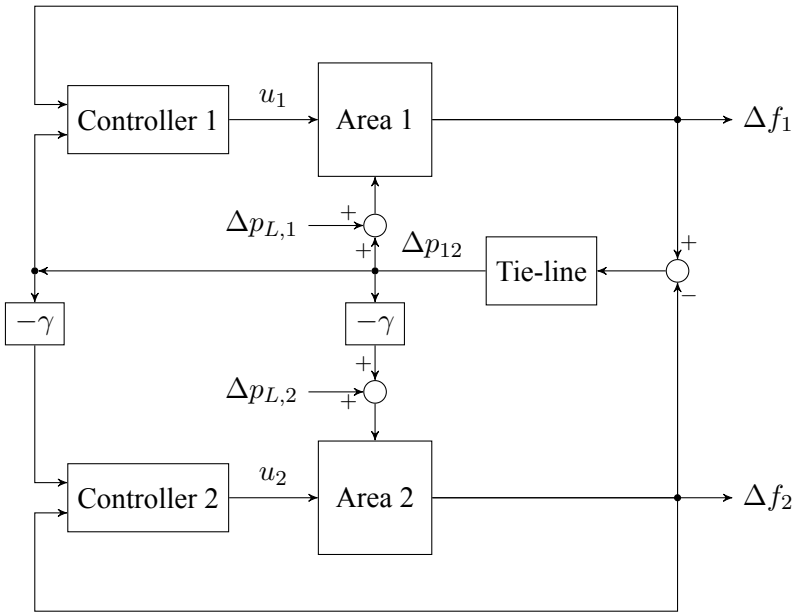

u_i is the control signal of Area i $\Delta p_{L,i}$ is the load deviation in Area i

Δf_i is the frequency deviation of Area i Δp_{12} is the tie-flow (from Area 1 to Area 2)

γ is the ratio of the base power between Area 1 and Area 2 $\left(\gamma = \dfrac{\text{Base Power of Area 1}}{\text{Base Power of Area 2}}\right)$

Figure 2.4: Block diagram of LFC for two-area interconnected power system

sharing of the power between the areas are achieved.

In this regard, the term 'area control error' (ACE), which is the sum of the net tie-flow deviation and the product of the frequency deviation with a bias constant, has been introduced (see, e.g., [28, 29] and the references therein) and being used as an input signal of LFC for interconnected power system in order that the supplementary control in a given area should ideally correct only for change in that area.

$$\text{ACE}_i = \Delta p_{e,i} + B_i \Delta f_i \tag{2.3}$$

where ACE_i is the ACE signal of Area i, $\Delta p_{e,i}$ the deviation of the net tie-flow exchange of

Area i, B_i the bias factor of Area i, and Δf_i the frequency deviation of Area i.

It is well known (see, e.g., [22, 36] and the references therein) that a centralized controller requires information (or state variables) of every interconnected area to generate the control signal. Thus, the implementation possesses difficulty especially if there is large number of areas. For this reason, decentralized control schemes, in which each area can then be controlled separately by a local controller, have been developed by many researchers (see, e.g., [3, 12, 15–17, 20, 41]).

The block diagram of LFC for two-area interconnected power system is shown in Figure 2.4. It is noted that the block 'Area i' may be illustrated as in Figure 2.2.

2.2.3 Generation Rate Constraint (GRC)

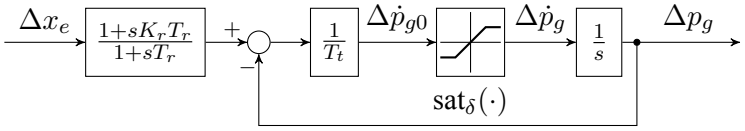

Δx_e is the input (the governor valve position) Δp_g is the output (the generated power)

$\Delta\dot{p}_{g0}$ is the unsaturated generation rate $\Delta\dot{p}_g$ is the generation rate

K_r, T_r, and T_t are the parameters of the turbine

Figure 2.5: Block diagram of reheat steam turbine

In practice, a generator is known to have a limitation on how fast the power output can be generated; this is especially the case for generators of reheat steam turbine type [34]. The limitation is imposed to avoid wide variations of process variables (e.g., temperature, pressure, etc.) for safety purposes. This is known as a generation rate constraint (GRC), which is an important constraint to be taken into account in formulating the LFC problem [34].

The GRC can be represented as a saturation function of the generation rate variable as shown in Figure 2.5. The saturation function $\text{sat}_\delta(\cdot)$ is defined by

$$\text{sat}_\delta(v) \triangleq \begin{cases} \delta \ \text{sgn}(v) & |v| > \delta, \\ v & |v| \leq \delta \end{cases} \tag{2.4}$$

where δ is a positive number called saturation level and $\text{sgn}(\cdot)$ denotes the signum function defined by

$$\text{sgn}(v) \triangleq \begin{cases} -1 & \text{if } v < 0, \\ 0 & \text{if } v = 0, \\ 1 & \text{if } v > 0. \end{cases} \tag{2.5}$$

This is obvious that, when the GRC is taken into the account, the system consists of a static nonlinear characteristic (see, e.g., [26] for details). Therefore, the linearization technique is not applicable.

It is important to note that in spite of having the nonlinear characteristic (2.4), the turbine shown in Figure 2.5 can be treated as a linear system as long as the signal $|\Delta\dot{p}_{g0}(t)| \leq \delta$ for all time t. According to the notion of conditionally linear system [42], the inequality

$$|\Delta\dot{p}_{g0}(t)| \leq \delta \qquad \text{for all } t \text{ and for all possible disturbances} \tag{2.6}$$

is incorporated in the design formulation. Consequently, only linear systems theory will be used in the analysis and the design.

2.3 Battery Energy Storage System (BESS)

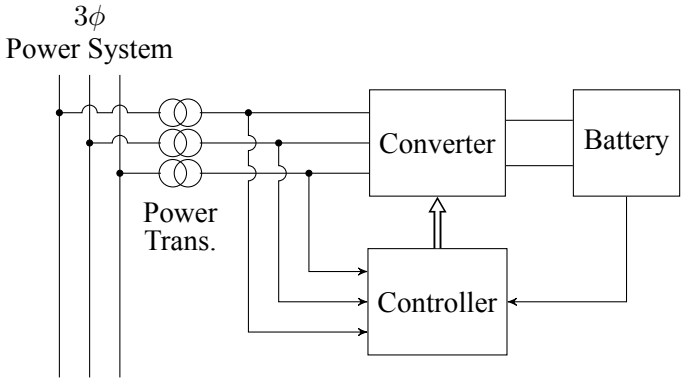

Figure 2.6: Schematic description of a BESS [32]

Battery energy storage system (BESS) is a system that helps in storing and supplying energy to the system. There are many applications of BESS, for examples [1],

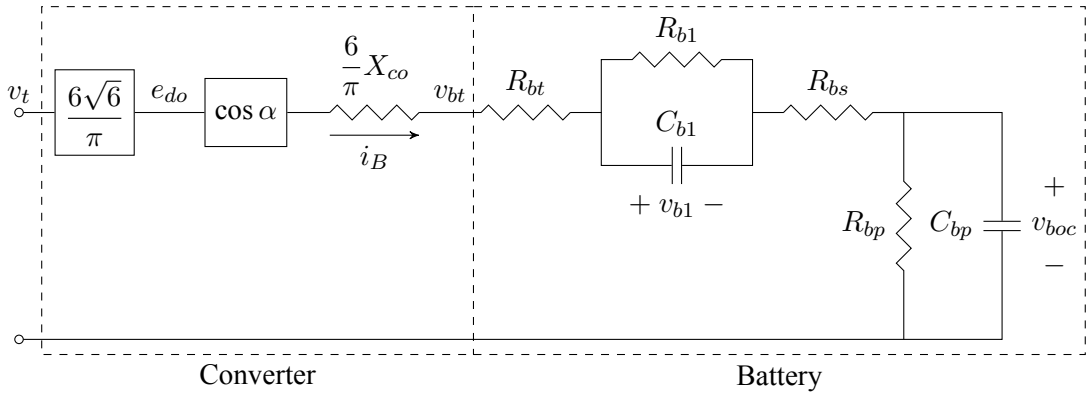

Figure 2.7: Equivalent circuit of a BESS [32]

- load shifting, BESS shifts wind energy from night to peak hour;
- uninterrupted power supply, BESS supplies power when source fails;
- power quality improvement, BESS minimizes the voltage sags;
- frequency regulation, BESS regulates frequency when wind farm is connected to the grid.

In this thesis, the BESS for frequency regulation is considered.

The equivalent configuration of a BESS (for frequency regulation) is shown in Figure 2.6. The main components of the BESS are a battery bank, a power conditioning equipment (converter), a transformer, and a controller.

A dynamic model of a BESS for a large-scale power system stability is developed in [31]. Since the thesis considers LFC problems, only some aspect of the BESS is taken into account. The dynamic model of the BESS for LFC used in the thesis is taken from References [2, 32]. The derivation is summarized as follows.

The ideal no-load maximum DC voltage of the converter is expressed as

$$e_{do} = e_{do1} + e_{do2} = 2 \times \frac{3\sqrt{6}}{\pi} v_t \tag{2.7}$$

where v_t is the line to neutral rms voltage. The terminal voltage of the equivalent battery is

obtained from

$$\begin{aligned} v_{bt} &= e_{do}\cos\alpha - R_c i_B \\ &= \frac{3\sqrt{6}}{\pi} v_t \left(\cos\alpha_1 + \cos\alpha_2\right) - \frac{6}{\pi} X_{co} i_B \end{aligned} \tag{2.8}$$

where

X_{co} is the commutating reactance,

i_B the DC current flowing into the equivalent battery, and

α_i the firing delay angle of converter i.

The equivalent circuit of the BESS can be represented as a converter connected to an equivalent battery (Figure 2.7) with the same cosine value of the firing delay angles in (2.8) where

v_{boc} is the battery open-circuit voltage,

v_{b1} the battery overvoltage,

R_{bt} the connecting resistance,

R_{bs} the internal resistance,

R_{b1} the overvoltage resistance,

C_{b1} the overvoltage capacitance,

R_{bp} the self discharge resistance, and

C_{bp} the battery capacitance.

The expression of the DC current flowing into the battery can be obtained from the equivalent circuit analysis as

$$i_B = \frac{v_{bt} - v_{boc} - v_{b1}}{R_{bt} + R_{bs}} \tag{2.9}$$

where

$$\begin{aligned} v_{boc} &= \frac{R_{bp}}{1 + sR_{bp}C_{bp}} i_B \\ v_{b1} &= \frac{R_{b1}}{1 + sR_{b1}C_{b1}} i_B. \end{aligned} \tag{2.10}$$

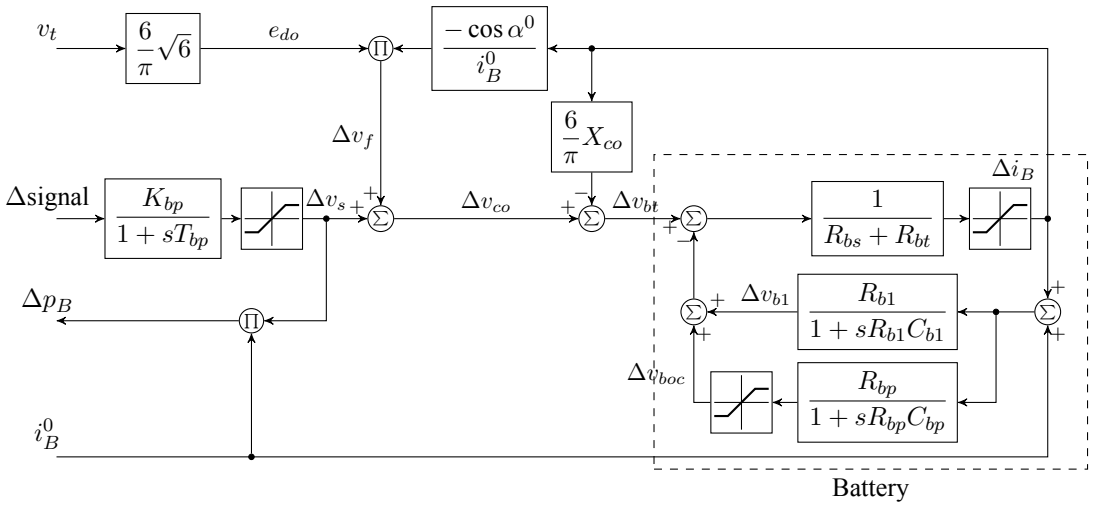

Figure 2.8: Block diagram of BES incremental model

According to the converter circuit analysis [27], the real and reactive power absorbed by (charged to) the BESS are

$$\begin{aligned} p_B &= \frac{3\sqrt{6}}{\pi} v_t i_B \left(\cos\alpha_1 + \cos\alpha_2\right) \\ q_B &= \frac{3\sqrt{6}}{\pi} v_t i_B \left(\sin\alpha_1 + \sin\alpha_2\right). \end{aligned} \tag{2.11}$$

There are two control strategies: namely,

1. P-Q modulation $(\alpha_1 = \alpha_2 = \alpha)$

$$\begin{aligned} p_B &= \frac{6\sqrt{6}}{\pi} v_t i_B \left(\cos\alpha\right), \\ q_B &= \frac{6\sqrt{6}}{\pi} v_t i_B \left(\sin\alpha\right); \end{aligned} \tag{2.12}$$

2. P modulation $(\alpha_1 = -\alpha_2 = \alpha)$

$$\begin{aligned} p_B &= \frac{6\sqrt{6}}{\pi} v_t i_B \left(\cos\alpha\right) \\ &= e_{do} I_B \cos\alpha = v_{co} i_B, \\ q_B &= 0 \end{aligned} \tag{2.13}$$

where $v_{co} = e_{do}\cos\alpha$ is the DC voltage without overlap. Since only incremental active power is considered in load frequency control, the P modulation is used in this work. Linearization of (2.13) yields the incremental power of the BESS

$$\Delta p_B = v_{co}^0 \Delta i_B + i_B^0 \Delta v_{co}. \tag{2.14}$$

Although the constant current operating mode is the most efficient for BESS, the BESS should operate in constant power mode for the sake of LFC. Thus, the firing angle α (in the term Δv_{co}) is adjusted. The term Δv_{co} is decomposed into two components: (i) Δv_f to compensate the power deviation caused by Δi_B, and (ii) Δv_s to respond the system disturbance. By assuming that

$$\Delta v_f = \frac{-e_{do}\cos\alpha^0}{i_B^0}\Delta i_B, \tag{2.15}$$

one can obtain

$$\begin{aligned}\Delta p_B &= v_{co}^0\Delta i_B + i_B^0\left(\Delta v_f + \Delta v_s\right)\\ &= i_B^0\Delta v_s.\end{aligned} \tag{2.16}$$

Then the use of the BESS in LFC is obtained by a damping signal Δv_s

$$\Delta v_s = \frac{K_{bp}}{1+sT_{bp}}\Delta\text{signal} \tag{2.17}$$

where K_{bp} and T_{bp} are the control loop gain and the measurement device time constant, respectively. The Δsignal is a useful feedback from the power system in order to provide damping effect. By combining the above equations (2.7), (2.8), (2.9), (2.10), (2.15), (2.16) and (2.17), the incremental model of the BESS can be represented in Figure 2.8.

The discharging mode operation of the BESS can also be represented by Figure 2.8. One can use the ignition angle β for the converter in discharging mode [27]. The power consumption of the BESS is

$$\begin{aligned}\Delta p_B &= \frac{6\sqrt{6}}{\pi}v_t i_B\cos\beta \qquad (\beta = \pi - \alpha)\\ &= -e_{do}i_B\cos\alpha = -v_{co}i_B.\end{aligned} \tag{2.18}$$

Similar to the charging mode, the incremental power of BESS for discharging mode is obtained.

$$\Delta p_B = -i_B^0\Delta v_s. \tag{2.19}$$

The operating mode (charging or discharging) of the incremental BESS model shown in Figure 2.8 depends on the sign of i_B^0 value, which indicates the direction of initial current within the BESS. Since there are DC breakers to prevent too high currents which would endanger batter service life, the deviation of battery current is limited. There is also a limit upon Δv_s due to $v_{co} \le e_{do}$.

$C_{bp} = 52597$ F	$R_{bp} = 10$ kΩ	$C_{b1} = 1$ F	$R_{b1} = 0.01\ \Omega$
$R_{bt} = 0.0167\ \Omega$	$R_{bs} = 0.013\ \Omega$	$X_{co} = 0.0274\ \Omega$	$i_B^0 = \pm 4.426$ kA
$\alpha^0 = 15^\circ$	$\beta^0 = 25^\circ$	$K_{bp} = 100$ kV/Hz	$T_{bp} = 0.026$ s

Table 2.1: Parameters for a 10 MW/40 MWh BESS

For simplicity, the operation of the BESS for LFC used in the thesis can be represented as in Figure 2.9 where Δsignal is the feedback signal from the power system, Δp_b is the power of the BESS (depended on the mode of operation), $K_b = K_{bp} i_B^0 / P_r$, $T_b = T_{bp}$, and P_r is the rated power of the system. The parameters (taken from [2, 32]) are given in Table 2.1.

Note that Δp_b indicates the power absorbing from the system if it is in the charging mode and thus i_B^0 has a positive value. If the discharging mode is assumed, Δp_b indicates the power supplying to the system and i_B^0 has a minus sign.

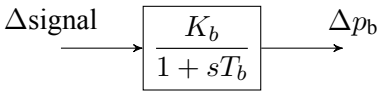

Figure 2.9: Simplified model of BESS used in the thesis

CHAPTER III

FUNDAMENTAL DESIGN THEORY

This chapter briefly reviews the design theories that are used in the thesis. The design methodology known as Zakian's framework and the fundamental theory associated with the framework involved are presented.

3.1 Reviews of Zakian's Framework

Zakian's framework consists of two design principles: namely, the principle of inequalities [42, 44, 46] and the principle of matching [42–44]. On the one hand, the principle of inequalities suggests that a multiobjective design problem should be cast as a set of inequalities that can be solved in practice. On the other hand, the principle of matching suggests what kind of inequalities should be used in order the design formulation is appropriate in the sense that the control objectives can be effectively achieved. This section provides a brief review of the framework. The details of the framework are gathered and presented in [45].

3.1.1 Principle of Inequalities

Zakian [44–46] advocates that any design theory must provide a mathematical way of characterizing a good design. It has long been recognized that a good design is usually specified by means of several criteria that are required to be satisfied simultaneously.

The principle of inequalities provides a way of formulating control problems appropriately. This principle asserts that a design problem should be formulated as a set of inequalities

$$\phi_i(\mathbf{p}) \leq C_i \quad (i = 1, 2, \ldots, r) \tag{3.1}$$

where $\mathbf{p} \in \mathbb{R}^n$ is a vector of design parameters, $\phi_i : \mathbb{R}^n \to \mathbb{R} \cup \{\infty\}$ represents a quality or a property or an aspect of the behavior of the system, and the numbers C_i is the largest value of ϕ_i that can be accepted. Any point $\mathbf{p}$ satisfying (3.1) characterizes an acceptable design solution.

Following the principle of inequalities, it is important to note [44–46] that the set of inequalities (3.1) includes two principal subsets, one subset representing constraints and the other

representing required performance. Whereas constraints have traditionally been represented by inequalities, the representation of desired performance by a set of inequalities is a significant departure from the tradition in which the performance is represented by a single objective function to be minimized. The principle of inequalities stated by means of several distinct criteria, with each criteria represented by one or more inequalities, thus allowing greater insight into the design process. In most cases, some of the principal ϕ_i are non-convex functions of the design parameter $\mathbf{p} \in \mathbb{R}^n$. Consequently, a numerical algorithm is usually employed to determine a solution of the equalities (3.1) by searching in the parameter space $\mathbb{R}^n$.

3.1.2 Principle of Matching

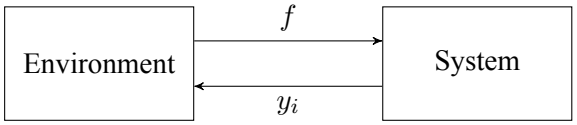

Figure 3.1: The relation between the environment and the system

The principle of matching is a general concept which requires that the system and the environment should be designed so that both are matched in the sense defined as follows [43–45].

Assume that the environment subjects the system to an input f which causes responses (or output) y_i $(i = 1, 2, 3, \ldots, m)$ in the system. Assume also that the input f generated by the environment is known to the extent that it belongs to a set $\mathcal{P}$, called the *possible set* [42–44]. This set comprises all inputs that can happen or are likely to happen or are allowed to happen in practice. The input f is said to be *tolerable* [42–44] if every output y_i $(i = 1, 2, 3, \ldots, m)$ satisfies

$$\|y_i(f, \mathbf{p})\|_\infty \leq \varepsilon_i \tag{3.2}$$

where ε_i is a positive number. The *tolerable set* $\mathcal{T}$ is defined as the set of all inputs that are tolerable. An environment and a system are said to be *matched* if every possible input is tolerable; that is, if the possible set $\mathcal{P}$ is a subset of the tolerable set $\mathcal{T}$.

Note that the notation $\|\cdot\|_\infty$ is defined by

$$\|z\|_\infty \triangleq \sup\{|z(t)| \mid t \in \mathbb{R}\} \tag{3.3}$$

and the tolerable set $\mathcal{T}$ can be expressed as

$$\mathcal{T} \triangleq \{f \mid \|y_i(f, \mathbf{p})\|_\infty \leq \varepsilon_i, \quad i = 1, 2, 3, \ldots, m\}. \tag{3.4}$$

A necessary and sufficient condition for the environment and the system to be matched is that the outputs corresponding to the possible input satisfy the following criteria:

$$\hat{y}_i(\mathbf{p}) \leq \varepsilon_i \quad (i = 1, 2, 3, \ldots, m) \tag{3.5}$$

where $\hat{y}_i$ is called the *peak output* corresponding to the possible set $\mathcal{P}$ and defined by

$$\hat{y}_i(\mathbf{p}) \triangleq \sup\{\|y_i(f, \mathbf{p})\|_\infty \mid f \in \mathcal{P}\}. \tag{3.6}$$

The criteria (3.5) are in keeping with the principle of inequalities and become useful design specifications, provided that $\hat{y}_i$ is computable (see §3.2.1). Accordingly, the design problem is usually to determine any value of $\mathbf{p} \in \mathbb{R}^n$ that satisfies (3.5).

3.2 Fundamental Control Theory

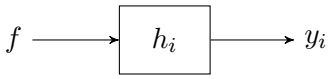

Figure 3.2: System whose input and output are related by convolution integral

This section provides the fundamental control theory associated with Zakian's framework. Consider a linear, time-invariant and non-anticipative system (Figure 3.2) whose input f and outputs y_i $(i = 1, 2, 3, \ldots, m)$ are related by the convolution integral

$$y_i(t, f, \mathbf{p}) = \int_{-\infty}^{\infty} h_i(t - \tau, \mathbf{p}) f(\tau) d\tau \tag{3.7}$$

where $h_i(\cdot, \mathbf{p})$ denotes the impulse response of the output y_i and depends on the design parameter $\mathbf{p} \in \mathbb{R}^n$. Throughout the thesis, suppose that the impulse response h_i of the system takes the form

$$h_i(t, \mathbf{p}) = \beta_i \delta(t) + h_i^1(t, \mathbf{p}) \tag{3.8}$$

where β_i is a real number, δ denotes the impulse (or Dirac delta) function and $h_i^1 : \mathbb{R} \to \mathbb{R}$ is a bounded and piecewise continuous function.

In addition, consider the possible set $\mathcal{P}$ which is characterized by

$$\mathcal{P} \triangleq \left\{ f \;\middle|\; \|f\|_\infty \leq \mathcal{M},\ \|\dot{f}\|_\infty \leq \mathcal{D} \right\} \tag{3.9}$$

where the bounds $\mathcal{M}$ and $\mathcal{D}$ are positive numbers that can be determined from the physical properties or the past records of the system. The set $\mathcal{P}$ given in (3.9) is noteworthy for the fact that it contains continuous signals that vary persistently for all time.

3.2.1 Computation of Performance Measures

The method proposed in [38] is used in the thesis for computing the peak outputs $\hat{y}_i$, defined in (3.6), in association with the possible set $\mathcal{P}$ characterized by (3.9). The method is summarized as follows.

The problem of computing $\hat{y}_i$ for (3.7) can be rewritten as

$$\hat{y}_i(\mathbf{p}) = \sup \{ J_i(f, \mathbf{p}) \mid f \in \mathcal{P} \} \tag{3.10}$$

where $J_i(f, \mathbf{p})$ is the performance measure defined by

$$J_i(f, \mathbf{p}) \triangleq \int_{-\infty}^{\infty} h_i(-\tau, \mathbf{p}) f(\tau) d\tau. \tag{3.11}$$

3.2.1.1 Performance measure approximation

It is shown in [38] that if the system is BIBO stable, then the improper integral in (3.11) is well approximated as

$$J_i(f, \mathbf{p}) \approx \beta_i f(0) + \int_{-T}^{T} h_i^1(-\tau, \mathbf{p}) f(\tau) d\tau, \quad T > 0, \tag{3.12}$$

for a sufficiently large T.

For $t \in [-T, T]$, the trajectories $h_i^1(t, \mathbf{p})$ and $f(t)$ are represented by the vectors $\mathbf{h}_i^1$ and $\mathbf{f}^0$ such that

$$\mathbf{h}_i^1 \triangleq \begin{bmatrix} h_i^{(-n_t)} & h_i^{(-n_t+1)} & h_i^{(-n_t+2)} & \dots & h_i^{(n_t-2)} & h_i^{(n_t-1)} & h_i^{(n_t)} \end{bmatrix}^{\mathrm{T}} \in \mathbb{R}^{2n_t+1} \tag{3.13}$$

and

$$\mathbf{f}^0 \triangleq \begin{bmatrix} f^{(-n_t)} & f^{(-n_t+1)} & f^{(-n_t+2)} & \dots & f^{(n_t-2)} & f^{(n_t-1)} & f^{(n_t)} \end{bmatrix}^{\mathrm{T}} \in \mathbb{R}^{2n_t+1}, \tag{3.14}$$

where $h_i^{(k)} \triangleq h_i^1(t_k, \mathbf{p})$ and $f_i^{(k)} \triangleq f_i(t_k)$. The time point t_k is given by

$$\begin{aligned} t_{-n_t} &= -T, \\ t_{k+1} &= t_k + \sigma, \quad \text{for } k = -n_t, -n_t+1, -n_t+2, \ldots, n_t-1, \end{aligned} \tag{3.15}$$

where the uniform difference $\sigma = T/n_t$ is used.

By setting the initial value of f to be zero (that is, $f^{(-n_t)} = 0$) so that the maximal input to be determined is unique, $\mathbf{f}^0$ in (3.14) is replaced by

$$\mathbf{f} \triangleq \begin{bmatrix} f^{(-n_t+1)} & f^{(-n_t+2)} & f^{(-n_t+3)} & \ldots & f^{(n_t-2)} & f^{(n_t-1)} & f^{(n_t)} \end{bmatrix}^{\mathrm{T}} \in \mathbb{R}^{2n_t}, \tag{3.16}$$

In this thesis, Simpson's rule is employed to compute the definite integral in (3.12). Let the positive number n_t be chosen to be even. It readily follows [38] that

$$\begin{aligned} J_i(f, \mathbf{p}) &\approx \left(\beta + \frac{\sigma}{3} h_i^{(0)}\right) f^{(0)} + \frac{\sigma}{3} \sum_{k=1}^{n_t-1} \left[3 + (-1)^{k+1}\right] h_i^{(n_t-k)} f^{(-n_t+k)} \\ &= \mathbf{c}_h^{\mathrm{T}} \mathbf{f} \quad \triangleq J_i(\mathbf{f}, \mathbf{p}), \end{aligned} \tag{3.17}$$

where the vector $\mathbf{c}_h \in \mathbb{R}^{2n_t}$ is given by

$$\mathbf{c}_h = \frac{\sigma}{3} \begin{bmatrix} 4h_i^{(n_t-1)} & 2h_i^{(n_t-2)} & \ldots & 4h_i^{(-1)} & \dfrac{3\beta}{\sigma} + h_i^{(0)} & \mathbf{0}_{1\times n_t} \end{bmatrix}^{\mathrm{T}}. \tag{3.18}$$

The zero subvector in (3.18) is a consequence of the non-anticipative property (that is, $h_i(t, \mathbf{p}) = 0 \; \forall t < 0$) of the system (3.7). Therefore, the performance measure $J_i(f, \mathbf{p})$ in (3.11) is approximated by $J_i(\mathbf{f}, \mathbf{p})$ in (3.17).

3.2.1.2 Constraints Approximation

Let $x \preceq y$ denotes componentwise inequality between vectors x and y. The inequality $\|f\|_\infty \leq \mathcal{M}$ can be replaced by

$$I\mathbf{f} \preceq \mathcal{M}\mathbf{1} \qquad \text{and} \qquad -I\mathbf{f} \preceq \mathcal{M}\mathbf{1} \tag{3.19}$$

where I denotes identity matrix and $\mathbf{1}$ denotes a vector with all components being one. Similarly, the inequality $\|\dot{f}\|_\infty \leq \mathcal{D}$ can be rewritten as

$$Q_d\mathbf{f} \preceq \mathcal{D}\mathbf{1} \qquad \text{and} \qquad -Q_d\mathbf{f} \preceq \mathcal{D}\mathbf{1} \tag{3.20}$$

where $Q_d \in \mathbb{R}^{2n_t \times 2n_t}$ is the matrix used in approximating the derivative by first-order forward difference formula and given by

$$Q_d = \frac{1}{\sigma} \begin{bmatrix} 1 & 0 & 0 & \cdots & 0 & 0 & 0 \\ -1 & 1 & 0 & \cdots & 0 & 0 & 0 \\ 0 & -1 & 1 & \cdots & 0 & 0 & 0 \\ \vdots & \vdots & \vdots & \ddots & \vdots & \vdots & \vdots \\ 0 & 0 & 0 & \cdots & 1 & 0 & 0 \\ 0 & 0 & 0 & \cdots & -1 & 1 & 0 \\ 0 & 0 & 0 & \cdots & 0 & -1 & 1 \end{bmatrix}. \tag{3.21}$$

Accordingly, the approximated peak output is the solution of the following optimization problem:

$$\begin{aligned} \max_{\mathbf{f}} \quad & J_i(\mathbf{f}, \mathbf{p}) \\ \text{subject to} \quad & \text{(3.19) and (3.20).} \end{aligned} \tag{3.22}$$

It is worth noting that the optimization problem in (3.22) has two important properties. First, it is guaranteed to be a convex problem for any difference $\sigma > 0$. Second, the matrices associated with (3.22) are sparse.

Nowadays, large-scale optimization problems can readily be solved by efficient numerical algorithms [45]. Therefore, the problem (3.22) can be solved efficiently in practice. In this thesis, the package called "SeDuMi" [39] is used to solved the problem (3.22).

3.2.2 Stabilization & Finiteness of Performance Measures

In solving the inequalities (3.5) by numerical methods, it is necessary to obtain a *stability point*, that is, a point $\mathbf{p} \in \mathbb{R}^n$ satisfying

$$\hat{y}_i(\mathbf{p}) < \infty \quad \text{for all } i. \tag{3.23}$$

This is because numerical search algorithms, in general, are able to seek a solution of (3.5) only if they start from such a point [42, 46]. Since the inequalities (3.23) are not soluble by numerical methods using only functions $\hat{y}_i$, one needs to replace (3.23) with equivalent (or practical sufficient) conditions that can be satisfied by numerical methods.

Assume that a state-space realization of the system is $\{A, B, C, D\}$. It is known (see, e.g., [38] and the references therein) that $\hat{y}_i(\mathbf{p}) < \infty$ for all i if and only if all the eigenvalues of A lie in the open left half of the complex plane; that is to say,

$$\alpha(\mathbf{p}) < 0 \tag{3.24}$$

where $\alpha(\mathbf{p})$ is called the *spectral abscissa* of A and defined as

$$\alpha(\mathbf{p}) \triangleq \max_i \mathrm{Re}\{\lambda_i(A)\} \tag{3.25}$$

and $\lambda_i(A)$ denotes an eigenvalue of A. Notice that $\alpha(\mathbf{p}) < \infty$ for all values of $\mathbf{p} \in \mathbb{R}^n$ and that the number α can be computed economically in practice.

In practice, the inequality (3.24) is usually replaced with

$$\alpha(\mathbf{p}) \leq -\varepsilon_0 \quad (0 < \varepsilon_0 \ll 1). \tag{3.26}$$

Accordingly, a stability point can readily be obtained by solving the inequality (3.26). It is noted that, once the stability point is obtained, the inequality (3.26) is used, during the search process, to prevent the algorithm from stepping out of the stability region.

CHAPTER IV

DESIGN OF LOAD FREQUENCY CONTROL FOR TWO-AREA POWER SYSTEM

This chapter presents the design of LFC for two-area interconnected power systems using Zakian's framework. The dynamic model of the power system used in this chapter is taken from Ćalović (1971), which is widely used by many researchers. The study carried out in this chapter illustrates that the framework can readily be applied to both SISO and MIMO design problems.

4.1 Dynamic Model of Two-Area Power Systems

A linearized state-space model of a two-area interconnected power system with mixed steam-hydro power generating units taken from [10, 11] is used, assuming small deviations of variables and separation of the real power and frequency behavior from the phenomena connected with reactive power and voltage. In addition, by neglecting the coupling effects among parallelly operated synchronous generating units within the same area, each area has a single frequency. The details of the model derivation can be found in [10].

The state-space representation of the LFC system of Area i is

$$\left.\begin{aligned} \dot{x}_{g,i} &= A_{g,i}x_{g,i} + B_{g,i}u_i + F_{g,i}z_i \\ y_{g,i} &= C_{g,i}x_{g,i} \end{aligned}\right\}, \qquad i = 1, 2. \tag{4.1}$$

The state vector of Area i is

$$x_{g,i} = \begin{bmatrix} \Delta a_{T,i} & \Delta p_{t1,i} & \Delta p_{t2,i} & \Delta p_{t3,i} & \Delta a_{H,i} & \Delta v_i & \Delta q_i & \Delta f_i \end{bmatrix}^{\mathrm{T}}$$

where

Δa	is the deviation of turbine valve (gate) opening, expressed in pu,
Δp_{t1}, Δp_{t2}, Δp_{t3}	the deviations of steam turbine high, intermediate and low-pressure outputs, respectively, expressed in pu,
Δv	the deviation of dashpot piston position relative to the lever of permanent speed droop of hydroturbine governor, expressed in pu,

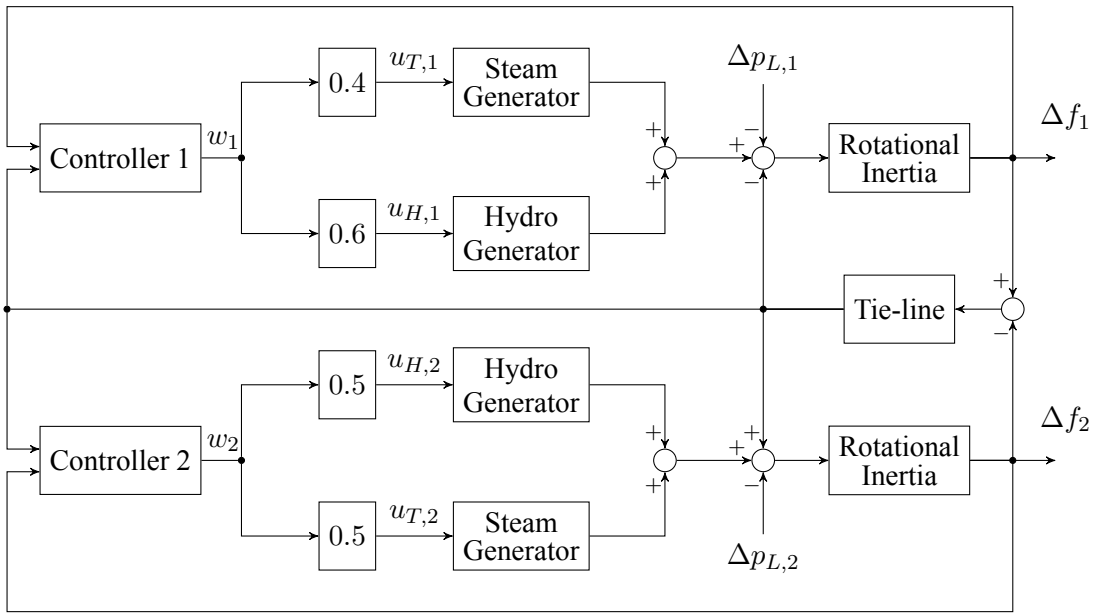

Figure 4.1: Block diagram of LFC for two-area interconnected power system which each area consists of steam and hydro generators

Δq	the deviation of hydroturbine flow, expressed in pu, and
Δf	the deviation of system frequency, expressed in pu.

Subscripts "T" and "H" designate the common parameters relative to steam units and hydro-units, respectively. For Area i, its control input vector is

$$u_i = [u_{T,i},\ \ u_{H,i}]^{\mathrm{T}},$$

and its disturbance is

$$z_i = \Delta p_{L,i}$$

where $\Delta p_{L,i}$ is the load deviation occurring in Area i. The output is

$$y_{g,i} = \Delta f_i.$$

The matrices $A_{g,i}$, $B_{g,i}$, $C_{g,i}$ and $F_{g,i}$ in (4.1) are constant and are given as follows.

$$A_{g,i} = \begin{bmatrix} -\frac{r_T}{T_{sT}} & 0 & 0 & 0 & 0 & 0 & 0 & -\frac{1}{T_{sT}} \\ \frac{k_t}{T_u} & -\frac{1}{T_u} & 0 & 0 & 0 & 0 & 0 & 0 \\ 0 & \frac{1}{T_r} & -\frac{1}{T_r} & 0 & 0 & 0 & 0 & 0 \\ 0 & 0 & \frac{1}{T_n} & -\frac{1}{T_n} & 0 & 0 & 0 & 0 \\ 0 & a_{52} & a_{53} & a_{54} & a_{55} & \frac{1}{T_{sH}} & a_{57} & a_{58} \\ 0 & 0 & 0 & 0 & \frac{r'}{T_e} & -\frac{1}{T_e} & 0 & 0 \\ 0 & 0 & 0 & 0 & \frac{1}{T_w} & 0 & -\frac{1}{T_q} & \frac{1}{T_f} \\ 0 & \frac{\epsilon_T c_v}{T} & a_{83} & a_{84} & -\frac{\epsilon_H k_w}{T} & 0 & \frac{\epsilon_H k_q}{T} & -\frac{e}{T} \end{bmatrix}_i,$$

$$B_{g,i}^{\mathrm{T}} = \begin{bmatrix} \frac{1}{T_{sT}} & 0 & 0 & 0 & 0 & 0 & 0 & 0 \\ 0 & 0 & 0 & 0 & \frac{1}{T_{sH}} & 0 & 0 & 0 \end{bmatrix}_i, \quad C_{g,i} = \begin{bmatrix} 0 & 0 & 0 & 0 & 0 & 0 & 0 & 1 \end{bmatrix},$$

$$F_{g,i}^{\mathrm{T}} = \begin{bmatrix} 0 & 0 & 0 & 0 & \frac{T_a}{TT_{sH}} & 0 & 0 & -\frac{1}{T} \end{bmatrix}_i$$

where

$$a_{52} = -\frac{\epsilon_T c_v T_a}{TT_{sH}}, \qquad a_{53} = -\frac{\epsilon_T c_s T_a (1-c_v)}{TT_{sH}},$$
$$a_{54} = -\frac{\epsilon_T T_a (1-c_v)(1-c_s)}{TT_{sH}}, \qquad a_{55} = \frac{1}{T_{sH}} \left(\frac{\epsilon_H k_w T_a}{T} - r_H - r' \right),$$
$$a_{57} = -\frac{\epsilon_H k_q T_a}{TT_{sH}}, \qquad a_{58} = \frac{eT_a - T}{TT_{sH}},$$
$$a_{83} = \frac{\epsilon_T c_s (1-c_v)}{T}, \qquad a_{84} = \frac{\epsilon_T (1-c_v)(1-c_s)}{T},$$

and the parameters are explained as follows.

r	steady-state speed droop
T_s	governor servomotor time constant
T_a	accelerometric time constant
T_e	dashpot time constant

$T_u,\ T_r,\ T_n$	time constants associated with steam turbine
k_t	proportionality factor
r'	transient speed droop
c_v	fraction of power developed by high pressure turbine relative to total unit power output
c_s	fraction of power developed by intermediate pressure turbine relative to total unit power output
$e_1,\ e_2,\ \ldots,\ e_{11}$	hydro-turbine non-dimensional coefficients
T	system acceleration time constant
e_p	consumer coefficient
e	system self-regulation coefficient
e_T	steam turbine self-regulation coefficient
ϵ	participation coefficient of particular unit in total system load
T_c	penstock time constant
$k_{i,j}$	tie-line capacity relative to the steady-state load
$(\theta_{i,j})_o$	initial phase angle difference between areas
f_o	steady-state frequency
m_s	synchronizing power flow coefficient

For the two-area interconnected LFC system (shown in Figure 4.1), the state equations are described by

$$\begin{aligned} \dot{x}_g &= A_g x_g + B_g u + F_g z \\ y_g &= C_g x_g. \end{aligned} \tag{4.2}$$

r	$=$	0.05 pu	T_{sT}	$=$	0.25 sec	T_{sH}	$=$	0.10 sec
T_a	$=$	0.80 sec	T_e	$=$	2.00 sec	T_u	$=$	0.20 sec
T_r	$=$	6.00 sec	T_n	$=$	0.50 sec	k_t	$=$	0.95
r'	$=$	0.40 sec	c_v	$=$	0.30	c_s	$=$	0.30
e_p	$=$	1.50 pu	e_T	$=$	0.15 pu	T_c	$=$	1.20 sec
ϵ_{T1}	$=$	0.40	ϵ_{H1}	$=$	0.50	ϵ_{L1}	$=$	0.10
ϵ_{T2}	$=$	0.50	ϵ_{H2}	$=$	0.40	ϵ_{L2}	$=$	0.10
e_1	$=$	0.60	e_2	$=$	0.95	e_3	$=$	0.07
e_4	$=$	0.18	e_5	$=$	$1+e_1+e_3$	e_6	$=$	e_2+e_4
e_7	$=$	$1-2e_1$	e_8	$=$	$e_2e_5-e_1e_6$	e_9	$=$	$1-2e_1-2e_3$
e_{10}	$=$	$e_5e_7-e_1e_9$	e_{11}	$=$	$-2e_3$	T	$=$	12.0 sec
$k_{1,2}$	$=$	0.10 pu	$(\theta_{1,2})_o$	$=$	$\pi/4$ rad	f_o	$=$	50.0 Hz
e	$=$	$e_p-\epsilon_T e_T+\epsilon_H e_H$	m_s	$=$	$2k_{1,2}\pi f_o\cos(\theta_{1,2})_o$			

Table 4.1: System parameters for LFC in Figure 4.1

where

$$x_g=\left[\begin{array}{c} x_{g,1} \\ \hline \Delta p_{12} \\ \hline x_{g,2} \end{array}\right],\quad u=\left[\begin{array}{c} u_1 \\ \hline u_2 \end{array}\right],\quad z=\left[\begin{array}{c} z_1 \\ \hline z_2 \end{array}\right],\quad y_g=\left[\begin{array}{cc|cc} y_{g,1} & \Delta p_{e,1} & y_{g,2} & \Delta p_{e,2} \end{array}\right]^{\mathrm{T}},$$

$$A_g=\left[\begin{array}{c|c|c} A_{g,1} & F_{g,1} & 0 \\ \hline M_s & 0 & -M_s \\ \hline 0 & -\gamma F_{g,2} & A_{g,2} \end{array}\right],\quad B_g=\left[\begin{array}{c|c} B_{g,1} & 0 \\ \hline 0 & 0 \\ \hline 0 & B_{g,2} \end{array}\right],\quad C_g=\left[\begin{array}{c|c|c} C_{g,1} & 0 & 0 \\ 0 & 1 & 0 \\ \hline 0 & 0 & C_{g,2} \\ 0 & -\gamma & 0 \end{array}\right],$$

$$F_g=\left[\begin{array}{c|c} F_{g,1} & 0 \\ \hline 0 & 0 \\ \hline 0 & F_{g,2} \end{array}\right],\quad M_s=\left[\begin{array}{cccccc|c} 0 & 0 & 0 & 0 & 0 & 0 & m_s \end{array}\right],\quad \gamma=\frac{P_{o,1}}{P_{o,2}}=1.$$

The system parameters are given in Table 4.1. Note that $\Delta p_{e,i}$ is the deviation of the net tie-flow exchange of Area i. For two-area interconnection, $\Delta p_{e,1}=\Delta p_{12}$ and $\Delta p_{e,2}=\Delta p_{21}=-\gamma\Delta p_{12}$.

4.2 Design Formulation

This section explains how the design problem is formulated for the case in which persistent load deviations are assumed to take place in both areas. Let the power system be subjected to the load deviations $\Delta p_L(t)$ for $t \geq 0$ where Δp_L is characterized by (3.9). The controller is to be designed to satisfy the specifications of LFC problem which are given in §4.2.2.

4.2.1 Control Configuration

For practical reasons, only the local frequency deviation and the tie-flow deviation are fed back to each local controller. Assume that the controller is described by the following state equations.

$$\begin{aligned} \dot{x}_k &= A_k x_k + B_k y_g \\ w &= C_k x_k + D_k y_g \\ u &= \nu w \end{aligned} \tag{4.3}$$

where $x_k = \left[x_{k,1}^{\mathrm{T}},\ x_{k,2}^{\mathrm{T}}\right]^{\mathrm{T}}$, $x_{k,i}$ is the state vector of Area i controller, w is the controller output, ν is the unit control participation matrix such that w_i is the control signal of Area i, and $u_i = [u_{T,i},\ u_{H,i}]^{\mathrm{T}}$ is the vector consisting of signals sent to the steam- and the hydro-units in Area i. The closed-loop system is therefore described by

$$\begin{aligned} \dot{x} &= Ax + Fz \\ y &= Cx \end{aligned} \tag{4.4}$$

where

$$A = \left[\begin{array}{c|c} A_g + B_g \nu D_k C_g & B_g \nu C_k \\ \hline B_k C_g & A_k \end{array}\right], \quad F = \left[\begin{array}{c} F_g \\ \hline 0 \end{array}\right], \quad C = \left[\begin{array}{c|c} C_g & 0 \end{array}\right], \quad x = \left[\begin{array}{c} x_g \\ \hline x_k \end{array}\right].$$

Because only the local frequency deviation and the tie-flow deviation are fed back to the controller, the matrices A_k, B_k, C_k and D_k in (4.3) take the following forms:

$$\begin{aligned} A_k &= \left[\begin{array}{c|c} A_{k,1} & 0 \\ \hline 0 & A_{k,2} \end{array}\right], \quad B_k = \left[\begin{array}{c|c} B_{k,1} & 0 \\ \hline 0 & B_{k,2} \end{array}\right], \\ C_k &= \left[\begin{array}{c|c} C_{k,1} & 0 \\ \hline 0 & C_{k,2} \end{array}\right], \quad D_k = \left[\begin{array}{c|c} D_{k,1} & 0 \\ \hline 0 & D_{k,2} \end{array}\right] \end{aligned} \tag{4.5}$$

where $\{A_{k,i},\ B_{k,i},\ C_{k,i},\ D_{k,i}\}$ is a state-space realization of the controller of Area i.

Note that there are a number of state-space representations that can be used for the controller. The one used here is a simple form and can be seen in §4.3.

4.2.2 Design Specifications

According to the principle of inequalities, the performance specifications are expressed as a set of inequalities that can be solved in practice. In the following, the specifications used in this case are explained.

1. The overall closed-loop system must be stable so that other performance measures are finite and thus can be evaluated. For this case (see §3.2.2), the system is stable if and only if

$$\phi_1(\mathbf{p}) \triangleq \alpha(\mathbf{p}) \leq -\varepsilon_0 \quad (0 < \varepsilon_0 \ll 1), \tag{4.6}$$

   where α is the spectral abscissa of A, defined in (3.25). In this case, $\varepsilon_0 = 1 \times 10^{-6}$ is used.

2. Following [18,19], both areas' frequency deviations due to change in load must lie within the standard frequency range of ± 200 mHz or $\pm 4 \times 10^{-3}$ pu. In this regard, the design specifications are

$$\phi_2(\mathbf{p}) \triangleq \Delta\hat{f}_1 \leq 4 \times 10^{-3} \text{ pu}, \tag{4.7}$$

$$\phi_3(\mathbf{p}) \triangleq \Delta\hat{f}_2 \leq 4 \times 10^{-3} \text{ pu}. \tag{4.8}$$

3. The incremental control signals Δw_1 and Δw_2 should remain within linear ranges of operation so as to ensure that the linear model is valid during the operation. In this case, the limits of ± 0.02 pu are used. Hence, this is fulfilled if

$$\phi_4(\mathbf{p}) \triangleq \Delta\hat{w}_1 \leq 2 \times 10^{-2} \text{ pu}, \tag{4.9}$$

$$\phi_5(\mathbf{p}) \triangleq \Delta\hat{w}_2 \leq 2 \times 10^{-2} \text{ pu}. \tag{4.10}$$

4. The tie-flow deviation due to change in load is minimized, leading to the design inequality

$$\phi_6(\mathbf{p}) \triangleq \Delta\hat{p}_{12} \leq q \tag{4.11}$$

where q is a positive number. With a starting value q_0, the minimal value of q is obtained by successively solving the inequalities (4.6)–(4.11) and gradually reducing q until no solution of the inequalities can be found.

It should be noted that, in this case, there are two inputs (or disturbances) in the system: namely, $\Delta p_{L,1}$ and $\Delta p_{L,2}$, the calculation for the peak output $\hat{y}_i$ due to both inputs is carried out by

$$\hat{y}_i = \hat{y}_{i,1} + \hat{y}_{i,2} \tag{4.12}$$

where $\hat{y}_{i,1}$ and $\hat{y}_{i,2}$ are the peak outputs of y_i caused only by the inputs $\Delta p_{L,1}$ and $\Delta p_{L,2}$, respectively.

Hence, the design problem to be solved is to determine a design parameter **p** which satisfies the inequalities (4.6)–(4.11) simultaneously. In this work, the search algorithm called the moving boundaries process (MBP) is used. For more details of the MBP algorithm, see [45,46]. It may be noted that other algorithms for solving inequalities may also be used. See, e.g., Chapters 7 and Chapter 8 of [45] and the references therein for details on this.

4.3 Numerical Results

The load deviations are assumed to be bounded by 0.01 pu of their scheduled values. The rate of change of the load deviations is bounded by 0.01 pu/s. Thus, in (3.9),

$$\mathcal{M} = 0.01 \text{ pu}, \qquad \mathcal{D} = 0.01 \text{ pu/s}. \tag{4.13}$$

For simplicity, the unit control participation matrix ν used here is a constant matrix and the same as in [11], in which the ratio of the load distribution to the steam and hydroplants is 2:3 for Area 1 and 1:1 for Area 2. Thus,

$$\nu = \begin{bmatrix} 0.4 & 0.6 & 0 & 0 \\ 0 & 0 & 0.5 & 0.5 \end{bmatrix}^{\mathrm{T}}. \tag{4.14}$$

It should be noted that, in this case, the system bias factor is allowed to be a design parameter to be determined as well.

Simple controller structures are tried first. The first attempt is the conventional PI controller that has the structure as in the dashed-box in Figure 4.2. The design parameters are p_1, p_2, p_3 for Area 1 controller, and p_4, p_5, p_6 for Area 2 controller with the same structure. It is easy to show that a minimal realization of the conventional PI controllers is as follows.

$$A_k = \left[\begin{array}{c|c} 0 & 0 \\ \hline 0 & 0 \end{array}\right], \qquad B_k = \left[\begin{array}{cc|cc} p_1 & 1 & 0 & 0 \\ \hline 0 & 0 & p_4 & 1 \end{array}\right],$$

$$C_k = \left[\begin{array}{cc|c} -p_3 & 0 & \\ \hline 0 & -p_6 & \end{array}\right], \qquad D_k = \left[\begin{array}{cc|cc} -p_1p_2 & 0 & 0 & 0 \\ \hline 0 & 0 & -p_3p_4 & 0 \end{array}\right].$$

After exhaustive searches, a design solution cannot be obtained. This may be because the conventional PI controller has the limitation such that the set of specifications described by (4.6)–(4.10) cannot be fulfilled. Thus, a more complex controller structure is used.

The final configuration of the controller is shown in Figure 4.2. It is clear that the configuration comprises conventional PI controllers using ACE signals plus second-order compensators using local frequency deviations. A minimal realization of the controller shown in Figure 4.2 is described as follows.

$$A_k = \left[\begin{array}{ccc|cc} -p_7 & -p_8 & 0 & 0 & 0 \\ 1 & 0 & 0 & 0 & 0 \\ 0 & 0 & 0 & 0 & 0 \\ \hline 0 & 0 & 0 & -p_{15} & -p_{16} \\ 0 & 0 & 0 & 1 & 0 \\ 0 & 0 & 0 & 0 & 0 \end{array}\right], \qquad B_k = \left[\begin{array}{cc|cc} 1 & 0 & 0 & 0 \\ 0 & 0 & 0 & 0 \\ p_1 & 1 & 0 & 0 \\ \hline 0 & 0 & 1 & 0 \\ 0 & 0 & 0 & 0 \\ 0 & 0 & p_9 & 1 \end{array}\right],$$

$$C_k = \left[\begin{array}{ccc|ccc} p_4(p_7-p_5) & p_4(p_8-p_6) & -p_3 & 0 & 0 & 0 \\ \hline 0 & 0 & 0 & p_{12}(p_{15}-p_{13}) & p_{12}(p_{16}-p_{14}) & -p_{11} \end{array}\right],$$

$$D_k = \left[\begin{array}{cc|cc} -(p_4+p_1p_2) & -p_2 & 0 & 0 \\ \hline 0 & 0 & -(p_{12}+p_9p_{10}) & -p_{10} \end{array}\right].$$

After a number of iterations, the MBP algorithm manages to locate a solution of the inequalities (4.6)–(4.11) where the least value of q that can be achieved is $q^\star = 2.76 \times 10^{-2}$ pu.

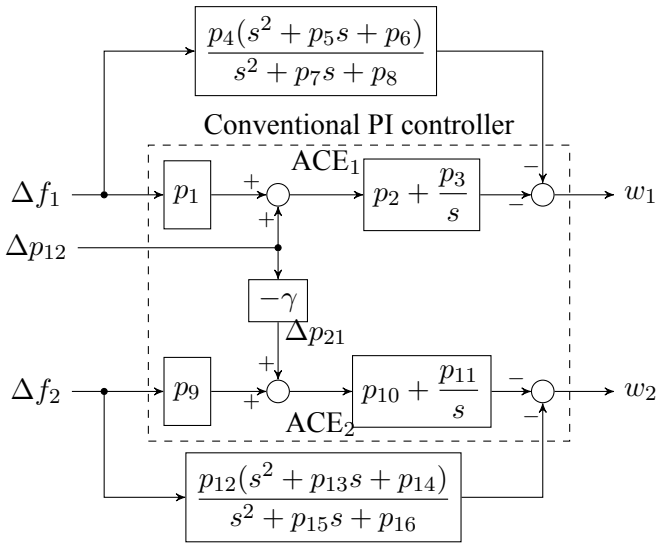

Figure 4.2: Controllers which consists of conventional PI controllers and compensators

The obtained design solution is

$$\mathbf{p}^\star = [p_1^\star,\ p_2^\star,\ p_3^\star,\ \ldots,\ p_{16}^\star]^{\mathrm{T}} \tag{4.15}$$

where

$$\begin{aligned}
&p_1^\star = 9.946, && p_2^\star = 2.349\times10^{-4}, && p_3^\star = 6.422\times10^{-3}, && p_4^\star = 41.92,\\
&p_5^\star = 4.120, && p_6^\star = 4.475\times10^{-2} && p_7^\star = 4.208, && p_8^\star = 36.65,\\
&p_9^\star = 4.563, && p_{10}^\star = 3.095\times10^{-1}, && p_{11}^\star = 6.388\times10^{-2}, && p_{12}^\star = 39.00,\\
&p_{13}^\star = 2.480, && p_{14}^\star = 1.250\times10^{-4}, && p_{15}^\star = 3.280, && p_{16}^\star = 27.33,
\end{aligned}$$

The corresponding performance measures are

$$\begin{aligned}
\phi_1(\mathbf{p}^\star) &= -5.386\times10^{-2} && < -1\times10^{-6},\\
\phi_2(\mathbf{p}^\star) &= 3.812\times10^{-3}\ \text{pu} && < 4\times10^{-3}\ \text{pu},\\
\phi_3(\mathbf{p}^\star) &= 3.428\times10^{-3}\ \text{pu} && < 4\times10^{-3}\ \text{pu},\\
\phi_4(\mathbf{p}^\star) &= 1.998\times10^{-2}\ \text{pu} && < 2\times10^{-2}\ \text{pu},\\
\phi_5(\mathbf{p}^\star) &= 1.964\times10^{-2}\ \text{pu} && < 2\times10^{-2}\ \text{pu},\\
\phi_6(\mathbf{p}^\star) &= 2.754\times10^{-2}\ \text{pu} && < 2.76\times10^{-2}\ \text{pu}.
\end{aligned} \tag{4.16}$$

To verify the design obtained in (4.15), the test inputs $\Delta p_{L,1}^\star$ and $\Delta p_{L,2}^\star$ in Figure 4.3 are used in the simulation. Note that both test inputs belong to the possible set $\mathcal{P}$ characterized by

the bounds $\mathcal{M}$ and $\mathcal{D}$ given in (4.13). The system variables Δf_1, Δf_2, Δw_1, Δw_2 and Δp_{12} in response to the disturbance vector $[\Delta p^{\star}_{L,1},\ \ \Delta p^{\star}_{L,2}]$ are displayed in Figure 4.4.

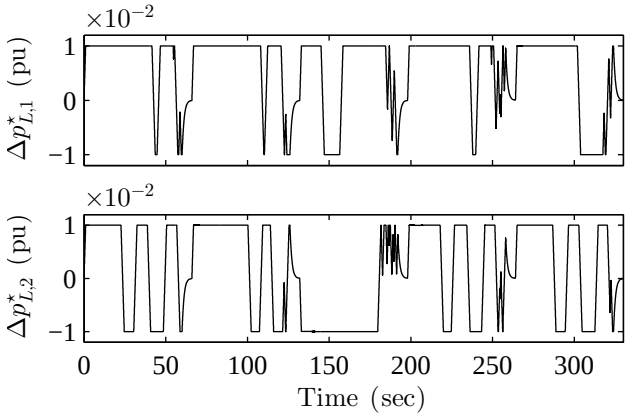

Figure 4.3: Test inputs used in the simulation for two-area interconnected power system

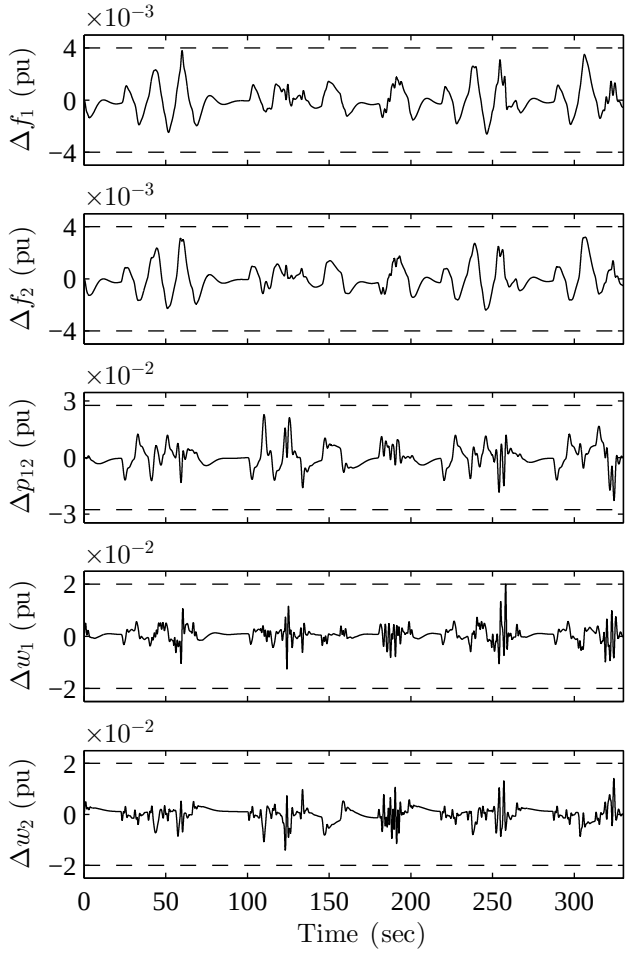

Figure 4.4: The system responses due to $\Delta p^{\star}_{L,1}$ and $\Delta p^{\star}_{L,2}$ with controller (4.15)

4.4 Conclusions

This chapter presents a general procedure for designing LFC for two-area power systems that are subject to bounded persistent disturbances. The disturbances are assumed to be taking place on both areas at the same time. Thus, the problem is considered as MIMO design problem. By using the framework adopted in the thesis, the results clearly show that all of the variables of interest strictly remain within the prescribed bounds and thus the objectives are achieved.

In the numerical results, the conventional controller (see Figure 4.2) which has a few design parameters is tried first. When the solution cannot be found, a more complex (higher order) controller is tried next. This is a practical means of finding an appropriate controller structure. Theoretically, there are many controller configurations that can be used. However, in practice, it is a good idea to preserve the conventional controller structure and add an extra compensator in order to reconstruct a higher order controller. Following this, the controller in Figure 4.2 is used in the case.

The case in which the GRC is taken into account will be considered in Chapter 5.

CHAPTER V

DESIGN OF LOAD FREQUENCY CONTROL CONSIDERING GENERATION RATE CONSTRAINT

The aim of this chapter is to design the LFC with the consideration of the GRC. Thus, the model of the power system used in this chapter is chosen to be a single area power system with reheat steam turbine. By using the principle of matching in conjunction with the notion of conditionally linear model, the LFC can be designed such that the generation rate variable can be kept within its linear range of operation. The disturbance is assumed to consist of two components: slow with large magnitude, and fast with small magnitude. In this regard, the BESS is used in the case to illustrate the effect of GRC on the system.

5.1 Dynamic Model of Single Area Power Systems

The dynamic model of a power system with a reheat thermal unit is used in this chapter. The generation rate constraint for the reheat unit is considered. The detailed transfer function models of speed governors and turbines are discussed and developed in [23]. For practical purposes, the models of the governor and the steam turbine used in this work are represented by first-order transfer functions. Also, assumptions of small deviations of variables and separation of the real power and frequency behavior from the phenomena connected with reactive power and voltage are made as usual.

In addition, the operating point of the BESS is assumed to be zero power output ($p_b^0 = 0$ pu) and the state of charge is neglected. Moreover, the BESS in this case is assumed to be operating in the discharging mode and the output of the BESS Δp_b indicates the power supplying to the system. Thus, the BESS gain K_b has a minus sign (see §2.3 for details).

The block diagram of the LFC overall system used in this chapter can be represented as in Fig. 5.1 where u is the control input, Δp_L is the disturbance deviation, and the state variables x_i $(i = 1, 2, 3, 4)$ are as follows:

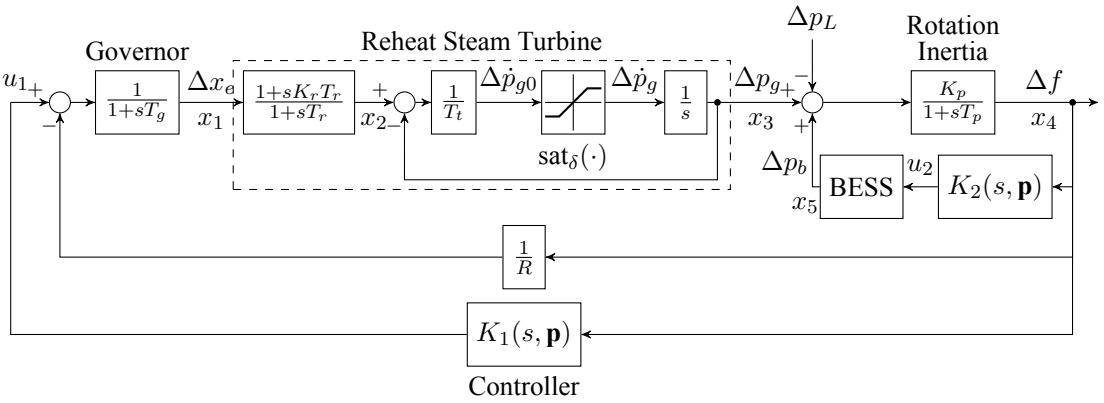

Figure 5.1: Block diagram of the single area LFC with BESS considering GRC

x_1 the governor valve position (Δx_e),

x_2 the state variable of the reheat steam turbine,

x_3 the power generation (Δp_g),

x_4 the frequency deviation (Δf), and

x_5 the power from BESS (Δp_b).

It is easy to verify that the LFC plant shown in Fig. 5.1 is described by the following state equations.

$$\begin{aligned}
\dot{x}_1(t) &= -\frac{1}{T_g}x_1(t) - \frac{1}{T_gR}x_4(t) + \frac{1}{T_g}u_1(t),\\
\dot{x}_2(t) &= \left(\frac{1}{T_r} - \frac{K_r}{T_g}\right)x_1(t) - \frac{1}{T_r}x_2(t) - \frac{K_r}{T_gR}x_4(t) + \frac{K_r}{T_g}u_1(t),\\
\dot{x}_3(t) &= \text{sat}_\delta\left(\frac{1}{T_t}x_2(t) - \frac{1}{T_t}x_3(t)\right),\\
\dot{x}_4(t) &= \frac{K_p}{T_p}x_3(t) - \frac{1}{T_p}x_4(t) + \frac{K_p}{T_p}x_5(t) - \frac{K_p}{T_p}\Delta p_L(t),\\
\dot{x}_5(t) &= -\frac{1}{T_b}x_5(t) + \frac{K_b}{T_b}u_2(t),\\
\Delta f(t) &= x_4(t)
\end{aligned} \tag{5.1}$$

where K_p, T_p, K_r, T_r, T_g, T_t, R, K_b, and T_b are the system parameters whose values are given in Table 5.1.

According to [34], the GRC of 10%/min is used here. From Figure 5.1, it is clear that

the power system considered contains a saturation element, which is a static nonlinear characteristic. However, if one can guarantee that the saturation is never reached, then the system can be considered to be linear; hence, the saturation is simply neglected and consequently only the linear control theories that are reviewed in §3.1.2 can be used to solve the design problem. This is known as the notion of *conditionally linear model* [42].

When $|\dot{x}_3(t)| \leq 10\%/\text{min}$ for all t, one easily sees that the plant in (5.1) becomes linear and is thus described by

$$\begin{aligned} \dot{x}_g(t) &= A_g x_g(t) + B_g u(t) + F_g \Delta p_L(t), \\ \Delta f(t) &= C_g x_g(t) \end{aligned} \tag{5.2}$$

where $x_g = [x_1,\ x_2,\ x_3,\ x_4,\ x_5]^{\mathrm{T}}$ is the state vector of the plant, and the matrices $A_g \in \mathbb{R}^{5\times 5}$, $B_g \in \mathbb{R}^5$, $F_g \in \mathbb{R}^5$, and $C_g \in \mathbb{R}^{1\times 5}$ are as follows.

$$A_g = \begin{bmatrix} -\frac{1}{T_g} & 0 & 0 & -\frac{1}{T_g R} & 0 \\ \left(\frac{1}{T_r} - \frac{K_r}{T_g}\right) & -\frac{1}{T_r} & 0 & -\frac{K_r}{T_g R} & 0 \\ 0 & \frac{1}{T_t} & -\frac{1}{T_t} & 0 & 0 \\ 0 & 0 & \frac{K_p}{T_p} & -\frac{1}{T_p} & \frac{K_p}{T_p} \\ 0 & 0 & 0 & 0 & -\frac{1}{T_b} \end{bmatrix}, \quad B_g = \begin{bmatrix} \frac{1}{T_g} & 0 \\ \frac{K_r}{T_g} & 0 \\ 0 & 0 \\ 0 & 0 \\ 0 & \frac{K_b}{T_b} \end{bmatrix}, \quad F_g = \begin{bmatrix} 0 \\ 0 \\ 0 \\ -\frac{K_p}{T_p} \\ 0 \end{bmatrix},$$

$$C_g = \begin{bmatrix} 0 & 0 & 0 & 1 & 0 \end{bmatrix}.$$

System gain,	$K_p = 120$ Hz/pu	System time constant,	$T_p = 20$ s
High pressure fraction,	$K_r = 0.50$	Reheat time constant,	$T_r = 10$ s
Governor time constant,	$T_g = 0.08$ s	Turbine time constant,	$T_t = 0.30$ s
Regulation of governor,	$R = 2.40$ Hz/pu	Saturation level of GRC,	$\delta = 1.667 \times 10^{-3}$
BESS gain,	$K_b = -0.2213$ pu/Hz	BESS time constant,	$T_b = 0.026$ s
Rated power,	$P_r = 2,000$ MW	Steady state frequency,	$f_0 = 60$ Hz

Table 5.1: System parameters for LFC in Figure 5.1

5.2 Design Formulation

This section explains how the design problem is formulated for the case in which the load deviates persistently for a long period of time with uniform bounds on magnitude and slope. The GRC is explicitly taken into the account as a design constraint. The 10 MW/40 MWh BESS is applied in this case whose model and its details can be found in §2.3. The controller is designed to fulfil the design specifications that are discussed in §5.2.2.

5.2.1 Control Configuration

In the subsequent design, an output feedback controller is used, where the frequency deviation Δf is fed back to the controller. Suppose that the controller is described by the following state-space representation:

$$\begin{aligned} \dot{x}_k(t) &= A_k x_k(t) + B_k \Delta f(t), \\ u(t) &= C_k x_k(t) + D_k \Delta f(t) \end{aligned} \tag{5.3}$$

where x_k is the state vector of the controller, and u is the controller output.

One can easily verify from (5.2) and (5.3) that the LFC overall system is described by

$$\begin{aligned} \dot{x}(t) &= Ax(t) + F\Delta p_L(t), \\ y(t) &= Cx(t) \end{aligned} \tag{5.4}$$

where $x \triangleq \left[x_g^{\mathrm{T}},\ x_k^{\mathrm{T}}\right]^{\mathrm{T}}$ denotes the state vector, $y \triangleq [\Delta f,\ \Delta \dot{p}_g,\ \Delta p_b]^{\mathrm{T}}$ denotes the output vector of interest, k is the total number of state variables of the controller, and the associated matrices $A \in \mathbb{R}^{(5+k)\times(5+k)}$, $F \in \mathbb{R}^{(5+k)}$, and $C \in \mathbb{R}^{3\times(5+k)}$ are given by

$$A = \left[\begin{array}{c|c} A_g + B_g D_k C_g^{\mathrm{T}} & B_g C_k^{\mathrm{T}} \\ \hline B_k C_g^{\mathrm{T}} & A_k \end{array}\right], \quad F = \left[\begin{array}{c} F_g \\ \hline 0 \end{array}\right],$$

$$C = \left[\begin{array}{ccccc|c} & & C_g & & & 0 \\ 0 & \frac{1}{T_t} & -\frac{1}{T_t} & 0 & 0 & 0 \\ 0 & 0 & 0 & 0 & 1 & 0 \end{array}\right].$$

5.2.2 Design Specifications

In connection with the theory described in §3.1.2, the design specifications used here are expressed as a set of inequalities that can be solved in practice. Such specifications are as follows.

1. The overall closed-loop system is required to be stable so that the performance measures (namely, the peak values of the frequency deviation and the generation rate) are finite and thus can be evaluated. For this case (see §3.2.2), the system is stable if and only if

$$\phi_1(\mathbf{p}) \triangleq \alpha(\mathbf{p}) \leq -\varepsilon_0 \quad (0 < \varepsilon_0 \ll 1), \tag{5.5}$$

   where α is the spectral abscissa of A, defined in (3.25). In this case, $\varepsilon_0 = 1 \times 10^{-6}$ is used.

2. According to [18, 19], the system frequency deviation is required to always lie within the standard frequency range of ± 50 mHz during the operation. For this reason, the second design specification is expressed as

$$\phi_2(\mathbf{p}) \triangleq \Delta\hat{f} \leq 5 \times 10^{-2} \text{ Hz}. \tag{5.6}$$

3. The magnitude of the generation rate $\Delta\dot{p}_g$ is required not to exceed 0.1 pu/min so that the linear model of the turbine generator is valid during the operation. In this regard, the third design specification is

$$\phi_3(\mathbf{p}) \triangleq \Delta\hat{\dot{p}}_g \leq 1.667 \times 10^{-3} \text{ pu/s}. \tag{5.7}$$

4. The magnitude of the power output from BESS Δp_b is limited by the rate of BESS. Since the 10 MW/40 MWh BESS is used and the rated power of the system is 2,000 MW, the power output of one unit of BESS is limited by 0.5×10^{-2} pu. Thus, the last inequality is set as

$$\phi_4(\mathbf{p}) \triangleq \Delta p_b \leq 0.5b \times 10^{-2} \text{ pu} \quad (b \in \{1,\ 2,\ 3,\ \dots\}) \tag{5.8}$$

   where b is an integer indicating the number of BESS units used. This inequality is chosen in such a way that the value of b starts with 1 and if the algorithm cannot find a solution $\mathbf{p}$ that satisfies inequalities (5.5), (5.6), (5.7), and (5.8), then we gradually increase the value of b until a solution is found.

Consequently, the design problem is to determine a design parameter vector **p** which satisfies the inequalities (5.5), (5.6), (5.7), and (5.8) simultaneously. Thus, for simplicity, the set of inequalities (5.5), (5.6), (5.7), and (5.8) is called the *main design inequalities*. Note that a search algorithm called the moving boundaries process (MBP) is used in this study; see [45, 46] for more details of the algorithm.

5.3 Numerical Results

This section presents the numerical results of the design problem formulated in §5.2. At this point, the possible set needs to be defined. In this case, to investigate some aspect in the power system, the possible disturbance is chosen in such a way that it contains large magnitude but slow signal and also small magnitude but fast signal.

The disturbance Δp_L in this case is assumed to consist of 2 components as follows:

$$\Delta p_L = \Delta p_{L,1} + \Delta p_{L,2} \tag{5.9}$$

where

$$\Delta p_{L,1} \in \mathcal{P}_1 \quad \triangleq \{x : \mathbb{R}_+ \to \mathbb{R} \mid \|x\|_\infty \leq \mathcal{M}_1,\ \|\dot{x}\|_\infty \leq \mathcal{D}_1\}, \tag{5.10}$$

$$\Delta p_{L,2} \in \mathcal{P}_2 \quad \triangleq \{x : \mathbb{R}_+ \to \mathbb{R} \mid \|x\|_\infty \leq \mathcal{M}_2,\ \|\dot{x}\|_\infty \leq \mathcal{D}_2\}, \tag{5.11}$$

and

$$\begin{aligned} \mathcal{M}_1 &= 2 \times 10^{-2} \text{ pu}, & \mathcal{M}_2 &= 3 \times 10^{-3} \text{ pu}, \\ \mathcal{D}_1 &= 1 \times 10^{-3} \text{ pu/s}, \quad \text{and} & \mathcal{D}_2 &= 1 \times 10^{-2} \text{ pu/s}. \end{aligned} \tag{5.12}$$

Clearly, the component $\Delta p_{L,1}$ represents a disturbance with a larger magnitude and a slower rate of change while $\Delta p_{L,2}$ represents a disturbance with a smaller magnitude and a faster rate of change. This suggests a more general situation in the power system in which the first component $\Delta p_{L,1}$ may represent the load change in a normal situation and the second component $\Delta p_{L,2}$ the power fluctuation from renewable energy sources (such as wind or sunlight).

An example of the disturbance characterized by (5.9) is shown in Figure 5.2. Note that this disturbance $\Delta p_L^\star$ will be used as a test input in subsequent simulations.

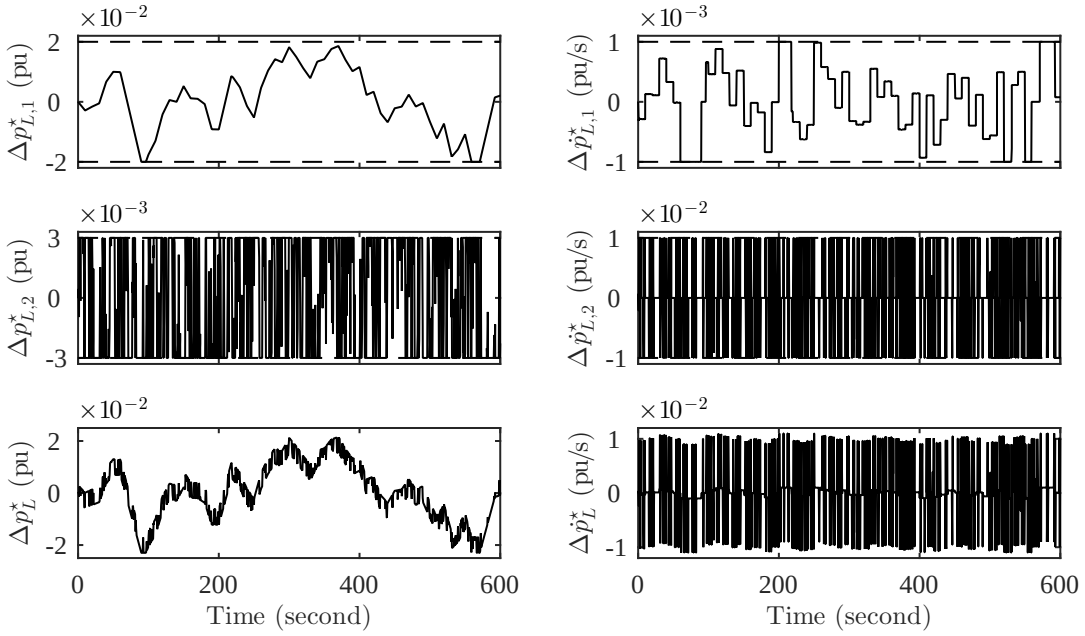

Figure 5.2: Test input used in the simulation for the power system with GRC

5.3.1 Case I

As usual, the simplest structure of the controller is tried first. The control structure is chosen to be a PI controller for the main loop and a unity gain feedback for the BESS loop. The design parameters vector is $\mathbf{p}^{(1)} \in \mathbb{R}^2$. Thus,

$$\begin{aligned} \mathbf{p}^{(1)} &\triangleq \left[p_1^{(1)},\ p_2^{(1)}\right]^{\mathrm{T}}, \\ K_1^{(1)}(s,\mathbf{p}^{(1)}) = p_1^{(1)} + \frac{p_2^{(1)}}{s}, &\quad \text{and} \quad K_2^{(1)}(s,\mathbf{p}^{(1)}) = 1. \end{aligned} \tag{5.13}$$

It is easy to show that a minimal realization of controller characterized by (5.13) is as follows.

$$A_k^{(1)} = 0, \qquad B_k^{(1)} = 1, \qquad C_k^{(1)} = \left[\frac{-p_2^{(1)}}{0}\right], \qquad D_k^{(1)} = \left[\frac{-p_1^{(1)}}{1}\right]. \tag{5.14}$$

After a number of iterations, the MBP algorithm cannot find the solution $\mathbf{p}^{(1)} \in \mathbb{R}^2$ that satisfies the main design inequalities. The best solution for which all the main design inequalities except the GRC are satisfied is obtained as follows.

$$\mathbf{p}^{(1)\star} = \left[1.000 \times 10^{-6},\ 5.472 \times 10^{-3}\right]^{\mathrm{T}}. \tag{5.15}$$

The corresponding performance measures are

$$\begin{aligned}
\alpha(\mathbf{p}^{(1)\star}) &= -8.632 \times 10^{-3}, \\
\Delta\hat{f}(\mathbf{p}^{(1)\star}) &= 3.632 \times 10^{-2} \text{ Hz}, \\
\Delta\hat{\dot{p}}_g(\mathbf{p}^{(1)\star}) &= 4.147 \times 10^{-3} \text{ pu/s} \quad > 1.667 \times 10^{-3} \text{ pu/s}, \\
\Delta\hat{p}_b(\mathbf{p}^{(1)\star}) &= 8.030 \times 10^{-3} \text{ pu} \quad (b = 2).
\end{aligned} \tag{5.16}$$

The system responses due to the test input $\Delta p_L^\star$ are depicted in Figure 5.3. Although all the outputs of interest can be kept within the acceptable bounds, one can obviously see that the generation rate variable $\Delta\dot{p}_g$ operates in the saturation region in which the assumption of linear model is violated and the computed peak outputs are not correct.

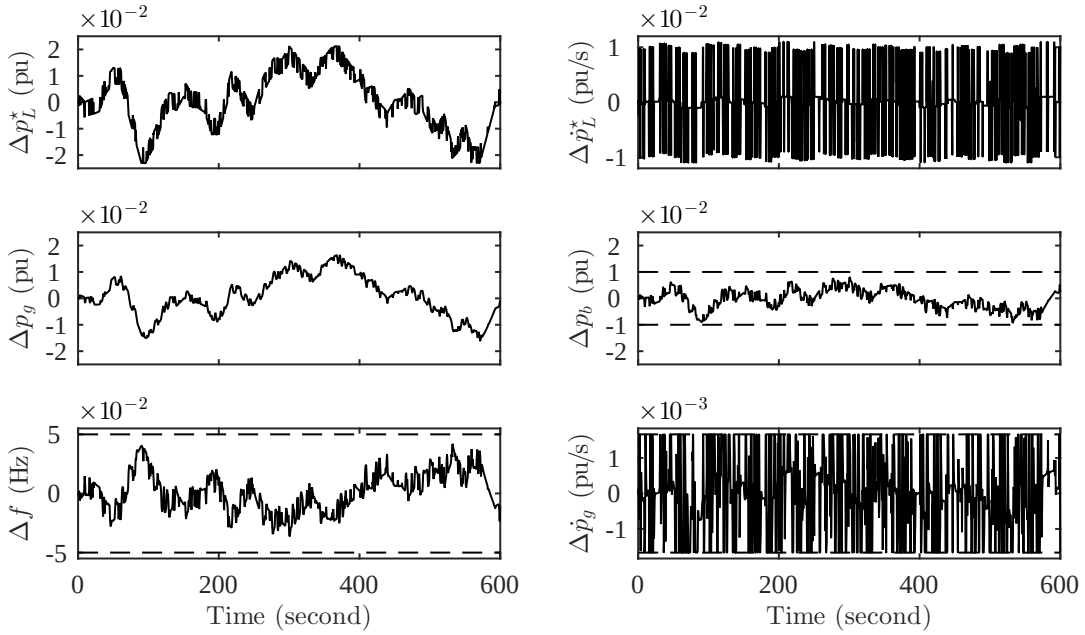

Figure 5.3: The system responses for Case I

5.3.2 Case II

Since the algorithm cannot find the design solution that satisfies the main design inequalities when the conventional controller in Case I is used, a more complex controller is tried next. In this case, a first-order compensator is cascaded with the PI controller in the main loop where the BESS loop remains using the unity gain. Then, the design parameters vector is $\mathbf{p}^{(2)} \in \mathbb{R}^4$.

Thus,

$$\begin{aligned}\mathbf{p}^{(2)} &\triangleq \left[p_1^{(2)},\ p_2^{(2)},\ p_3^{(2)},\ p_4^{(2)}\right]^{\mathrm{T}},\\ K_1^{(2)}(s,\mathbf{p}^{(2)}) &= p_1^{(2)}\left(\frac{s+p_2^{(2)}}{s}\right)\left(\frac{s+p_3^{(2)}}{s+p_4^{(2)}}\right), \quad \text{and} \quad K_2^{(2)}(s,\mathbf{p}^{(2)}) = 1.\end{aligned} \tag{5.17}$$

The minimal realization can be written as follows.

$$\begin{aligned}A_k^{(2)} &= \begin{bmatrix}-p_4^{(2)} & 0\\ 1 & 0\end{bmatrix}, \qquad B_k^{(2)} = \begin{bmatrix}1\\0\end{bmatrix},\\ C_k^{(2)} &= \begin{bmatrix}\dfrac{p_1^{(2)}(p_4^{(2)}-p_3^{(2)})-p_2^{(2)} & -p_2^{(2)}p_3^{(2)}}{0} & 0\end{bmatrix}, \qquad D_k^{(2)} = \begin{bmatrix}\dfrac{-p_1^{(2)}}{1}\end{bmatrix}.\end{aligned} \tag{5.18}$$

After exhaustive searches, the algorithm cannot find the solution $\mathbf{p}^{(2)} \in \mathbb{R}^4$ that satisfies our main design inequalities. Moreover, the best solution obtained is not significantly different from Case I, since all of the performance measures of both cases are similar. The solution obtained is

$$\mathbf{p}^{(2)\star} = \left[7.997\times10^{-7},\ 3.520\times10^{3},\ 6.663,\ 3.960\right]^{\mathrm{T}} \tag{5.19}$$

and the corresponding performance measures are

$$\begin{aligned}\alpha(\mathbf{p}^{(2)\star}) &= -7.457\times10^{-3},\\ \Delta\hat{f}(\mathbf{p}^{(2)\star}) &= 3.646\times10^{-2}\ \text{Hz},\\ \Delta\hat{p}_g(\mathbf{p}^{(2)\star}) &= 4.136\times10^{-3}\ \text{pu/s} \quad > 1.667\times10^{-3}\ \text{pu/s},\\ \Delta\hat{p}_b(\mathbf{p}^{(2)\star}) &= 8.058\times10^{-3}\ \text{pu} \quad (b=2).\end{aligned} \tag{5.20}$$

The system responses due to the test input $\Delta p_L^\star$ for this case are depicted in Figure 5.4. One can see that the system responses are very similar to those of Case I.

5.3.3 Case III

From Case II, one can see that the algorithm cannot find a better solution when a compensator is added to the main loop. This may be because the sensitivity of the BESS loop is not high enough. According to this, the controller for BESS loop is chosen to be a proportional gain

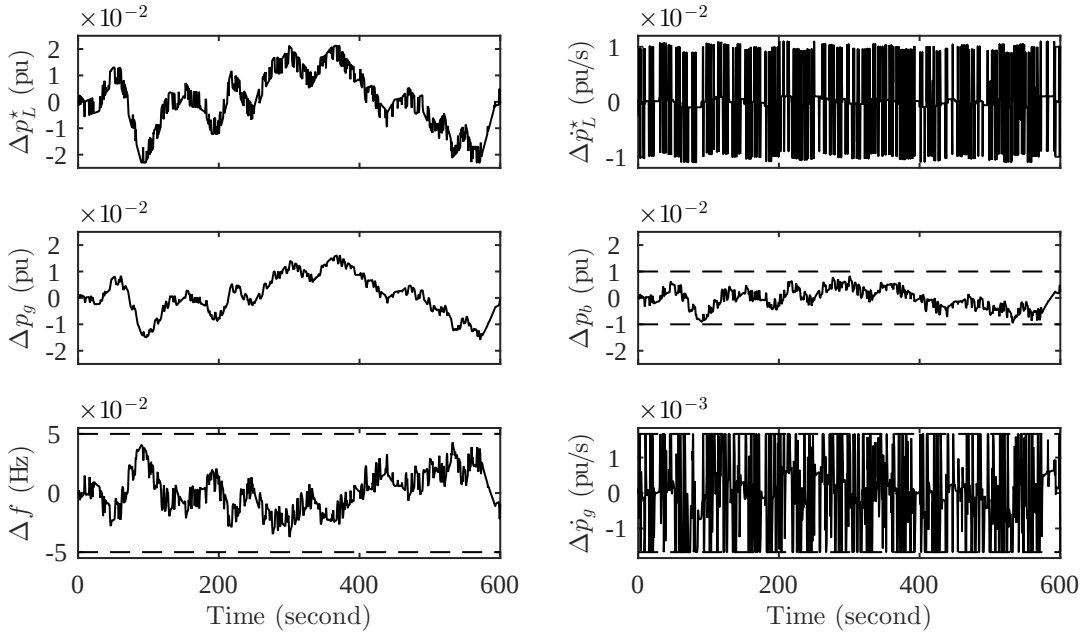

Figure 5.4: The system responses for Case II

while the main loop uses the PI controller. Now, the design parameters vector for Case III is $\mathbf{p}^{(3)} \in \mathbb{R}^3$ and

$$\begin{aligned} \mathbf{p}^{(3)} &\triangleq \left[p_1^{(3)},\ p_2^{(3)},\ p_3^{(3)}\right]^{\mathrm{T}}, \\ K_1^{(3)}(s,\mathbf{p}^{(3)}) &= p_1^{(3)} + \frac{p_2^{(3)}}{s}, \quad \text{and} \quad K_2^{(3)}(s,\mathbf{p}^{(3)}) = p_3^{(3)}. \end{aligned} \tag{5.21}$$

The minimal realization is given as

$$A_k^{(3)} = 0, \qquad B_k^{(3)} = 1, \qquad C_k^{(3)} = \begin{bmatrix} -p_2^{(3)} \\ \hline 0 \end{bmatrix}, \qquad D_k^{(3)} = \begin{bmatrix} -p_1^{(3)} \\ \hline p_3^{(3)} \end{bmatrix}. \tag{5.22}$$

For this case, after a number of iterations, the MBP algorithm manages to locate a solution $\mathbf{p}^{(3)} \in \mathbb{R}^3$ at

$$\mathbf{p}^{(3)\star} = \left[2.124,\ \ 10.17,\ \ 2.017 \times 10^2\right]^{\mathrm{T}}. \tag{5.23}$$

The performance measures are

$$\begin{aligned} \alpha(\mathbf{p}^{(3)\star}) &= -1.070 \times 10^{-1}, \\ \Delta\hat{f}(\mathbf{p}^{(3)\star}) &= 2.701 \times 10^{-4}\ \text{Hz}, \\ \Delta\hat{p}_g(\mathbf{p}^{(3)\star}) &= 1.635 \times 10^{-3}\ \text{pu/s}, \\ \Delta\hat{p}_b(\mathbf{p}^{(3)\star}) &= 1.152 \times 10^{-2}\ \text{pu} \qquad (b = 3). \end{aligned} \tag{5.24}$$

Finally, the algorithm can find a solution that satisfies the main design inequalities. The system responses are depicted in Figure 5.5.

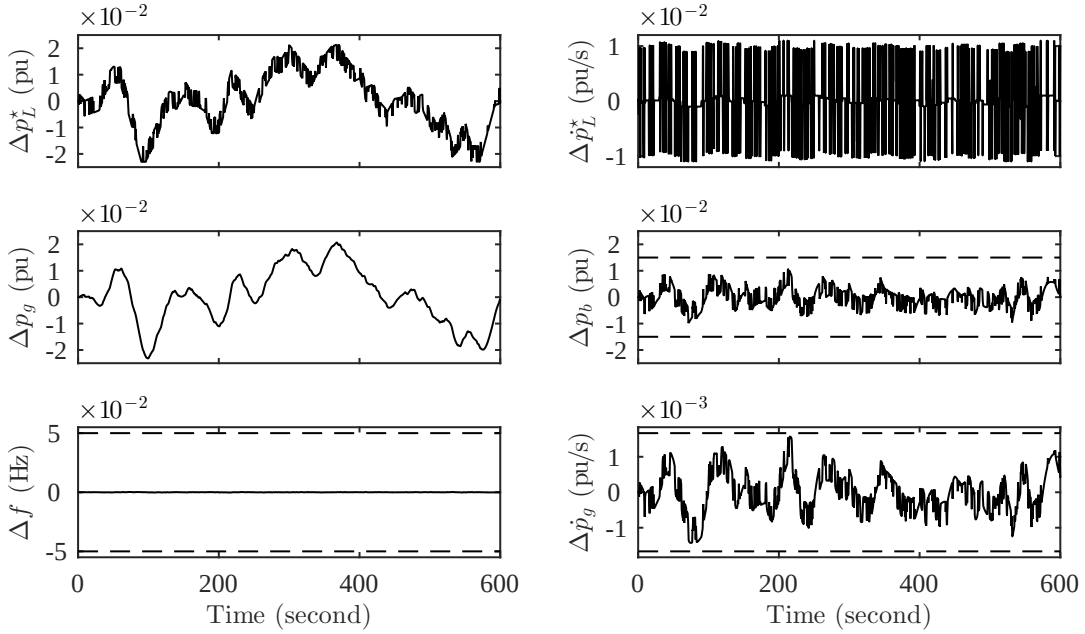

Figure 5.5: The system responses for Case III

5.3.4 Case IV

This case is set-up to illustrate the system responses of the situation when the system is operating without the BESS while the test input remains the same. The controller is chosen to be the conventional PI controller. Hence,

$$\begin{aligned} \mathbf{p}^{(4)} &\triangleq \left[p_1^{(4)},\ p_2^{(4)}\right]^{\mathrm{T}}, \\ K_1^{(4)}(s,\mathbf{p}^{(4)}) &= p_1^{(4)} + \frac{p_2^{(4)}}{s}, \quad \text{and} \quad K_2^{(4)}(s,\mathbf{p}^{(4)}) = 0. \end{aligned} \tag{5.25}$$

The minimal realization is as follows.

$$A_k^{(4)} = 0, \qquad B_k^{(4)} = 1, \qquad C_k^{(4)} = \begin{bmatrix} -p_2^{(4)} \\ \hline 0 \end{bmatrix}, \qquad D_k^{(4)} = \begin{bmatrix} -p_1^{(4)} \\ \hline 0 \end{bmatrix}. \tag{5.26}$$

The best solution in the sense that the peak value of the generation rate variable is lowest is

$$\mathbf{p}^{(4)\star} = \left[1.790 \times 10^{-7},\ 1.363 \times 10^{-3}\right]^{\mathrm{T}}. \tag{5.27}$$

The corresponding performance measures are

$$\begin{aligned} \alpha(\mathbf{p}^{(4)\star}) &= -3.212 \times 10^{-3}, \\ \Delta\hat{f}(\mathbf{p}^{(4)\star}) &= 6.593 \times 10^{-2}\ \text{Hz} \quad &> 5 \times 10^{-2}\ \text{Hz}, \\ \Delta\hat{\dot{p}}_g(\mathbf{4}^{(4)\star}) &= 6.529 \times 10^{-3}\ \text{pu/s} \quad &> 1.667 \times 10^{-3}\ \text{pu/s}, \\ \Delta\hat{p}_b(\mathbf{p}^{(4)\star}) &= 0\ \text{pu} \quad &(b = 0) \end{aligned} \tag{5.28}$$

and the system responses are presented in Figure 5.6.

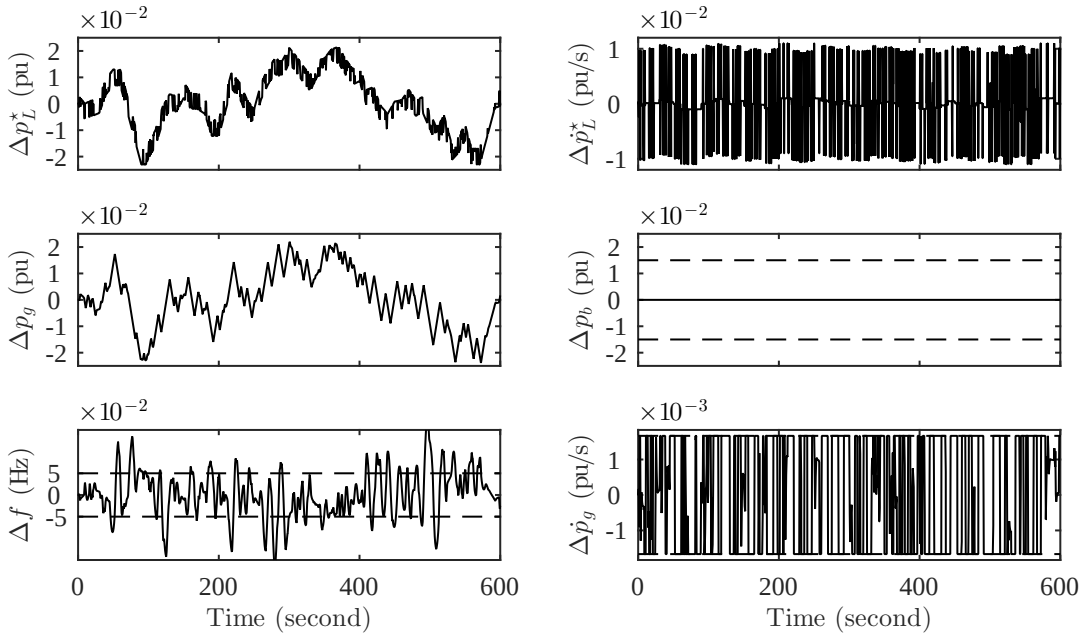

Figure 5.6: The system responses for Case IV

5.4 Conclusions

This chapter presents the design of LFC considering the GRC. The system under consideration is chosen to be a single area power system with a reheat steam turbine so that the model is simpler than the one used in Chapter 4. Thus, it is easier to study the effects of the GRC and of the BESS when the disturbance consists of two components, each of them representing persistent functions with different magnitude and different rate of change.

From the numerical results presented in §5.3, one can see that when the system is required to operate within a linear region, the limitation of the design is clearly shown on the generation rate variable $\Delta\dot{p}_g$.

- Case III is the only case in which the algorithm can find a design solution. It is evident that the effect of the fast changing component $\Delta p_{L,2}$ is eliminated by the action of the BESS. On the other hand, the effect of the slow component $\Delta p_{L,1}$ is eliminated largely by the action of the generator. In addition, from the simulation (see Figure 5.5), one can see that the BESS also handles some part of the effect caused by the slow component $\Delta p_{L,1}$. If one requires that the BESS should handle only the effect caused by the slow component and the generator handle only that caused by the fast component, then it may be necessary to add a high-pass filter into the BESS loop.

- For Case IV, it is obvious that, without the BESS, the system cannot achieve the satisfactory performance when the disturbance consists of the fast persistent component.

- For Case I and Case II, although the conditionally linear model is violated, the frequency deviation Δf from the simulation still remains within the acceptable range ± 50 mHz. This indicates that the system may also be able to operate satisfactorily in the saturation region. However, to design a controller for such cases, one needs a new theory for computing the peak values of the outputs for systems with such a nonlinear element, which unfortunately is not available at the time.

CHAPTER VI

CONCLUSIONS

6.1 Thesis Summary

This thesis describes a general procedure for designing a load frequency controller for power system subject to bounded persistent disturbances by using Zakian's framework, comprising the principle of inequalities and the principle of matching. The framework is effective and facilitates a realistic design formulation in the sense that the uncertain characteristics of the disturbances are explicitly taken into account. Moreover, by virtue of the framework, all the variables of interest are ensured to strictly remain within the prescribed bounds for all time and for all possible disturbances. Thus, the power system is guaranteed to operate with satisfactory levels of security and quality supply.

The generation rate constraint, which is caused by a saturation element in the system, is an important constraint on load frequency control problem. However, by using the principle of matching in conjunction with the notion of conditionally linear model, the load frequency control can be designed in such a way that the generation variable is kept within its linear range of operation. Consequently, linear control theories can be employed in solving the design problem; hence, nonlinear control theory is not needed.

In addition, when the generation rate constraint is considered with the presence of the load change caused by the use of renewable energy sources, the battery energy storage system can greatly improve the performance of the system. This is due to the fact that batteries can provide electrical energy much faster than rotating machines (generators). However, the generators are still the main generating units in electricity generation since they supply a much higher amount of electricity to the grid. Nowadays, nearly all of the electrical energy in the grid is provided by the generators.

6.2 Further Investigations and Possible Improvements

Some further investigations and possible improvements that are associated with this work and could be done are listed as follows.

1. In Chapter 5, the input to the battery energy storage system Δsignal is designed to be the frequency deviation multiplied by a proportional gain. However, it is possible to further design the Δsignal, e.g., by adding high-pass filter or first-order compensator, in order to obtain a better dynamic performances.

2. The framework adopted in the thesis can also be readily applied to the case of multi-area interconnected power systems.

3. In this work, when the generation rate constraint is considered, the system is restricted to operate only in linear region because at the moment only methods for computing peak outputs are available only for the case of linear system. However, if a new method for computing peak outputs of systems containing nonlinear elements were available, then the system could be allowed to operate in the saturation region and a better and less conservative result could be obtained. This suggests a subject for further investigation.

REFERENCES

[1] ABB group (2012). BESS overview - components, drivers, applications. IEEE PES meeting in Chicago, 8 February 2012.

[2] Aditya, S.K. and Das, D. (1999). Application of battery energy storage system to load frequency control of an isolated power system. International Journal of Energy Research, vol. 23, pp. 247–258.

[3] Alrifai, M.T., Hassan, M.F., and Zeibi, M. (2011). Decentralized load frequency controller for a multi-area interconnected power system. International Journal of Electrical Power & Energy Systems, vol. 33, pp. 189–209.

[4] Angeles-Camacho, C., Fariñas-Wong, E. and Bañuelos-Ruedas, F. (2010). FACTS: Its Role in the Connection of Wind Power to Power Networks. 2010 Proceedings of the International Symposium Modern Electric Power Systems (MEPS), Wrocław, Poland.

[5] Arunsawatwong, S. (1989). Decentralized Load-frequency Control of 2-area Power Systems via Output Feedback. Master's Thesis, Department of Electrical Engineering, Faculty of Engineering, Chulalongkorn University, Bangkok, Thailand.

[6] Arunsawatwong, S. (2013). Private communication.

[7] Arunsawatwong, S., Tia, K., and Eua-arporn, B. (2011). Design of static var compensator for power systems subject to voltage fluctuation satisfying bounding conditions. ECTI Transactions on Electronics and Communications, vol. 9, pp. 297–307.

[8] Bevrani, H., Ghosh, A., and Ledwich, G. (2010). Renewable energy sources and frequency regulation: survey and new perspectives. IET Renewable Power Generation, vol. 4, pp. 438–457.

[9] Boyd, S.P. and Barratt, C.H. (1991). Linear Controller Design: Limits of Performance. New Jersey: Prentice-Hall.

[10] Ćalović, M.S. (1971). Dynamic State-space Models of Electric Power Systems. Technical Report, Department of Electrical Engineering, Faculty of Engineering, University of Illinois.

[11] Ćalović, M.S. (1972). Linear regulator design for a load and frequency control. IEEE Transactions on Power Apparatus and Systems, vol. PAS-91, pp. 2271–2285.

[12] Ćalović, M.S. (1984). Automatic generation control: decentralized area-wise optimal solution. Electric Power Systems Research, vol. 7, pp. 115–139.

[13] Ćalović, M.S. (2012). Advanced automatic generation control with automatic compensation of tie-line losses. Electric Power Components and Systems, vol. 40, pp. 807–828.

[14] Chen, C.T. (1983). Linear System Theory and Design, 2nd ed. New York: Oxford University Press.

[15] Chidambaram, I.A. and Velusami, S. (2005). Design of decentralized biased controllers for load-frequency control of interconnected power systems. Electric Power Components and Systems, vol. 33, pp. 1313–1331.

[16] Davison, E.J. (1976). The robust decentralized control of a general servomechanism problem. IEEE Transactions on Automatic Control, vol. AC-21, pp. 14–24.

[17] Davison, E.J. and Tripathi, N.K. (1978). The optimal decentralized control of a large power system: load and frequency control. IEEE Transactions on Automatic Control, vol. AC-23, pp. 312–325.

[18] European Network of Transmission System Operators for Electricity (2013a). Network code on load-frequency control and reserves, 28 June 2013.

[19] European Network of Transmission System Operators for Electricity (2013b). Supporting document for the network code on load-frequency control and reserves, 28 June 2013.

[20] Feliachi, A. (1987). Optimal decentralized load frequency control. IEEE Transactions on Power Systems, vol. PWRS-2, pp. 379–385.

[21] Hussein, M.M., Senjyu, T., Orabi, M., Wahab, M.A., Hamada, M.M. (2013). Control of a stand-alone variable speed wind energy supply system. Applied Sciences, vol. 3, pp. 437–456.

[22] Ibraheem, I., Kumar, P., and Kothari, D.P. (2005). Recent philosophies of automatic generation control strategies in power systems. IEEE Transactions on Power Systems, vol. 30, pp. 346–357.

[23] IEEE Committee Report (1973). Dynamic models for steam and hydro turbines in power system studies. IEEE Transactions on Power Apparatus and Systems, vol. PAS-92, pp. 1904–1915.

[24] Kalvibool, P. and Arunsawatwong, S. (2014). Design of decentralized load frequency regulator for two-area power systems subject to bounded persistent disturbances. TENCON 2014 - 2014 IEEE Region 10 Conference. Bangkok, Thailand.

[25] Kalvibool, P. and Arunsawatwong, S. (2015). Design of load frequency regulator for power systems subject to bounded persistent disturbance considering generation rate constraint. 2015 54th Annual Conference of the Society of Instrument and Control Engineers of Japan (SICE), pp. 916–921. Hangzhou, China.

[26] Khalil, H.K., (2002). Nonlinear Systems, 3rd ed. New Jersey: Prentice Hall.

[27] Kimbark, E.W. (1971). Direct Current Transmission. New York: Wiley.

[28] Kothari, D.P. and Nagrath, I.J. (2012). Modern Power System Analysis. New Delhi: McGraw-Hill.

[29] Kundur, P. (1994). Power System Stability and Control. New York: McGraw-Hill.

[30] Lane, P.G. (1992). Design of Control Systems with Inputs and Outputs Satisfying Certain Bounding Conditions. PhD Thesis, University of Manchester Institute of Science and Technology, Manchester, United Kingdom.

[31] Lu, C.F., Liu, C.C., and Wu, C.J. (1995a). Dynamic modelling of battery energy storage system and application to power system stability. IEE Proceedings - Generation, Transmission and Distribution, vol. 142, pp. 429–435.

[32] Lu, C.F., Liu, C.C., and Wu, C.J. (1995b). Effect of battery energy storage system on load frequency control considering governor deadband and generation rate constraint. IEEE Transactions on Energy Conversion, vol. 10, pp. 555–561.

[33] Miniesy, S.M. and Bohn, E.V. (1972). Optimum load-frequency continuous control with unknown deterministic power demand. IEEE Transactions on Power Apparatus and Systems, vol. PAS-91, pp. 1910–1915.

[34] Nanda, J. and Kaul, B.L. (1978). Automatic generation control of an interconnected power system. Proceedings of the Institution of Electrical Engineers, vol. 125, pp. 385–390.

[35] Nidhiritdhikrai, R. (2006). Design of Automatic Generation Control Using the Method of Inequalities. Master's Thesis, Department of Electrical Engineering, Faculty of Engineering, Chulalongkorn University, Bangkok, Thailand.

[36] Pandey, S.K., Mohanty, S.R., and Kishor, N. (2013). A literature survey on load-frequency control for conventional and distribution generation power systems. Renewable and Sustainable Energy Reviews, vol. 25, pp.318–334.

[37] Reinelt, W. (2000). Maximum output amplitude of linear systems for certain input constraints. Proceedings of the 39th IEEE Conference on Decision and Control, pp. 1075-1080. Sydney, Australia.

[38] Silpsrikul, W. and Arunsawatwong, S. (2010). Computation of peak output for inputs satisfying many bounding conditions on magnitude and slope. International Journal of Control, vol. 83, pp. 49–65.

[39] Sturm, J.S. (1999). Use SeDuMi 1.02, a MATLAB toolbox for optimization over symmetric cones. Optimization Method and Software, vol. 11 & 12, pp 625–653.

[40] Tia, K., Arunsawatwong, S., and Eua-arporn, B. (2009). Design of compensators for power systems operating under load voltage fluctuation satisfying bounding conditions. 6th International Conference on Electrical Engineering/Electronics, Computer, Telecommunications and Information Technology (ECTI-CON), pp. 252–255. Pattaya, Thailand.

[41] Venkateswarlu, K. and Mahalanabis, A.K. (1977). Design of decentralised load-frequency regulators. Proceedings of the Institution of Electrical Engineers, vol. 124, pp. 817–820.

[42] Zakian, V. (1979). New formulation for the method of inequalities. Proceedings of the Institution of Electrical Engineers, vol. 126, pp. 579–584.

[43] Zakian, V. (1991). Well matched systems. IMA Journal of Mathematical Control and Information, vol. 8, pp. 29–38.

[44] Zakian, V. (1996). Perspectives on the principle of matching and the method of inequalities. International Journal of Control, vol. 65, pp. 147–175.

[45] Zakian, V. (2005) Control Systems Design: A New Framework. London: Springer-Verlag.

[46] Zakian, V. and Al-Naib, U. (1973). Design of dynamical control systems by the method of inequalities. Proceedings of the Institution of Electrical Engineers, vol. 120, pp. 1421–1427.

BIOGRAPHY

Patipan Kalvibool was born in Bangkok, Thailand on October 26, 1988. He obtained his Bachelor degree in electrical engineering from Chulalongkorn University, Thailand, in 2011. In 2012, he started his Master's study and did his research at Control System Research Laboratory, Department of Electrical Engineering, Faculty of Engineering, Chulalongkorn University, Thailand.

Throughout the undergraduate and graduate studies, his research was under the supervision of Assistant Professor Suchin Arunsawatwong. His research interest includes power system stability and control and computer aided design of control systems. In connection with his thesis, he has the following publications.

1. Kalvibool, P. and Arunsawatwong, S. (2014). Design of decentralized load frequency regulator for two-area power systems subject to bounded persistent disturbances. *TENCON 2014 - 2014 IEEE Region 10 Conference*. Bangkok, Thailand.
2. Kalvibool, P. and Arunsawatwong, S. (2015). Design of load frequency regulator for power systems subject to bounded persistent disturbance considering generation rate constraint. *2015 54th Annual Conference of the Society of Instrument and Control Engineers of Japan (SICE)*, pp. 916–921. Hangzhou, China.